Exhibit I
Part 1

Accepted Manuscript

In Vivo Oxidative Degradation of Polypropylene Pelvic Mesh

Adam Imel, Thomas Malmgren, Mark Dadmun, Samuel Gido, Jimmy Mays

PII: S0142-9612(15)00760-7

DOI: 10.1016/j.biomaterials.2015.09.015

Reference: JBMT 17065

To appear in: *Biomaterials*

Received Date: 3 May 2015

Revised Date: 3 September 2015

Accepted Date: 9 September 2015

Please cite this article as: Imel A, Malmgren T, Dadmun M, Gido S, Mays J, *In Vivo* Oxidative Degradation of Polypropylene Pelvic Mesh, *Biomaterials* (2015), doi: 10.1016/j.biomaterials.2015.09.015.

In Vivo Oxidative Degradation of Polypropylene Pelvic Mesh

Adam Imel[1], Thomas Malmgren[1], Mark Dadmun[1], Samuel Gido[2,*], Jimmy Mays[1,*]

[1]Department of Chemistry, University of Tennessee, Knoxville, TN 37996

[2]Department of Polymer Science and Engineering, University of Massachusetts, Amherst, MA 01003

*Corresponding authors: Samuel Gido, email gido@mail.pse.umass.edu, fax 413 545 0082; Jimmy Mays, email jimmymays@utk.edu, fax 865 974 9304

Abstract:

Commercial polypropylene pelvic mesh products were characterized in terms of their chemical compositions and molecular weight characteristics before and after implantation. These isotactic polypropylene mesh material showed clear signs of oxidation by both Fourier-transform infrared spectroscopy and scanning electron microscopy with energy dispersive X-ray spectroscopy (SEM/EDS). The oxidation was accompanied by a decrease in both weight-average and z-average molecular weights and narrowing of the polydispersity index relative to that of the non-implanted material. SEM revealed the formation of transverse cracking of the fibers which generally, but with some exceptions, increased with implantation time. Collectively these results, as well as the loss of flexibility and embrittlement of polypropylene upon implantation as reported by other workers, may only be explained by *in vivo* oxidative degradation of polypropylene.

Keywords: polypropylene; oxidation; degradation, SEM (scanning electron microscopy); molecular weight

Introduction

Polypropylene has been used as a mesh for hernia repair since 1958 [1], as well as in a wide variety of other biomaterials applications [2]. Because polypropylene is a hydrophobic polymer with no readily hydrolyzable bonds, surgeons have traditionally viewed it as an inert material *in vivo* [3]. However, as a member of the alkane family, with tertiary hydrogens on every other carbon in the backbone, polypropylene is susceptible to oxidative degradation [4]. In 1976, Liebert et al. studied in vivo degradation of polypropylene sutures in hamsters and using Fourier Transform infrared spectroscopy (FTIR), gel permeation chromatography (GPC), and mechanical properties measurements, saw clear evidence for oxidative degradation for polypropylene containing only a trace of antioxidant [5]. When higher loadings of a hindered phenolic antioxidant and a sulfur containing synergist were used, oxidation was suppressed on the time frame of the experiments (up to 100 days) [5]. Importantly, degradation of the polypropylene with trace antioxidant occurred at a much faster rate than one would expect for thermo-oxidative degradation under physiological conditions. Leibert et al. speculated that trace metals, enzymes or other chemicals present in the fluids might be responsible for the accelerated oxidative degradation [5]. It is now well-known that strong oxidizing agents such as hypochlorous acid and hydrogen peroxide are generated as byproducts of the inflammatory response of the body to an implant, and these agents can degrade and embrittle polypropylene, with a loss of flexibility due to oxidation selectively removing the less dense amorphous regions of the material [6]. These agents are believed to be responsible for the much faster than expected degradation of polypropylene *in vivo*. Polyethylene in orthopedic applications is also known to undergo degradation by an oxidative mechanism [7].

Recently several groups have reported *in vivo* degradation of polypropylene hernia meshes [8-10] and pelvic meshes [11]. Based on experiments in which degraded explanted polypropylene PP fibers in hernia meshes from various manufacturers were extracted with hexane, Bracco et al. [8] postulated that the primary cause of the cracked and degraded morphology of the fibers was their absorption of small organic molecules of biological origin including cholesterol, squalene, and esterified fatty acids. Referring to SEM images that showed obvious transverse cracking, they concluded that "In all the PP excised mesh fragments listed in Table 1 (Fig. 2 and Fig. 3), independently of the manufacturer or the implantation time, the filaments appear badly damaged."

Costello et al. [9,10] studied explanted polypropylene hernia meshes (from C. R. Bard and Ethicon) by a variety of techniques and concluded that cracks and other surface degradations such as peeling of the fibers were indicative of the oxidation of the polypropylene. They also remarked "Polypropylene is highly susceptible to the oxidative effects of the metabolites produced by phagocytic cells during the inflammatory response" and "…polypropylene is susceptible to oxidation, resulting from exposure to strong oxidants such as hydrogen peroxide and hypochlorous acid. These byproducts of the inflammatory response may degrade and embrittle the material, causing it to become rigid." Degradation causes surface cracking, mesh contraction, loss of mass, embrittlement, decreased melting temperature, foreign body reactions and reduced compliance of the material. They observed the explanted polypropylene fibers using scanning electron microscopy (SEM) and noted that micrographs of 79% of all explanted specimens exhibited cracks in the transverse or longitudinal direction. Clave et al. [11] studied explanted polypropylene pelvic meshes, observed degradation and cracking of the fibers, and concluded that polypropylene as a reinforcement in pelvic surgery is not inert. Their work was

with 71 different explanted PP meshes of various types from various manufacturers. These included low density monofilament, high density monofilament, multifilament, non-knitted non-woven, and composite PP meshes. All these different types showed cracking by SEM after implantation. However, their FTIR results neither confirmed nor excluded oxidation of polypropylene as the cause of the degradation.

Lefranc et al. [12] concluded the PP fiber meshes degrade when implanted for pelvic wall support, and cited transverse cracking as observed by SEM on explants as a characteristic identifier of this degradation. Lefranc [Ref. 12, Fig. 25.9] published a dramatic image of this cracking in explanted PP fibers, which he attributes to Clave, but which was not published in Clave's study [11].

Thus, while it is now becoming clear that polypropylene hernia and pelvic meshes, from a variety of manufacturers and of various types, are not inert *in vivo*, there still appears to be some uncertainty in the clinical community regarding the mechanism of degradation. The purpose of this study is to characterize explanted polypropylene pelvis meshes and compare their structure and properties with those of equivalent non-implanted materials. A combination of FTIR, GPC, SEM with energy dispersive X-ray spectroscopy (EDS), transmission electron microscopy (TEM), and thermogravimetric analysis (TGA) is used for this purpose.

Materials and Methods

Materials: Testing was performed to examine properties of explanted Boston Scientific Corporation Pinnacle and Obtryx pelvic repair meshes. Explanted samples of polypropylene mesh removed from 11 patients were received from Steelgate Inc. The samples were preserved in glass jars of formalin. Only 4 of the specimens contained sufficient amounts of polypropylene

mesh to allow for GPC and FTIR testing. However, SEM and EDS was performed on all 11 samples.

The properties of non-implanted samples of the Pinnacle and Obtryx products were compared to explanted samples of the same products to determine how polymer molecular weight, polymer chemical structure, polymer elemental composition, and the physical appearance of the fibers changed during implantation. Five other Boston Scientific pelvic meshes were also characterized via FTIR and GPC: Advantage Fit Transvaginal Mid-Urethral Sling System, Lynx Suprapubic Mid-Urethral Sling System, Prefyx PPS PrePubic System, Solyx SIS System, and Uphold Vaginal Support System. Four commercial polypropylene resins, Exxon Achieve 6936G1, Exxon PP3155, Metocene 500 MFR, and Metocene MF6504, used to make polypropylene fibers and non-woven fabrics were obtained from Dr. Gajanan Bhat in the Textiles and Nonwovens Development Center (TANDEC) at the University of Tennessee.

Fourier Transform Infrared Spectroscopy (FTIR)

FTIR spectra were obtained on PP meshes using a ThermoScientific Nicolet iS10 instrument. The PP meshes were folded (using gloves) and placed directly on top of the IR beam for scanning. Pellets of commercial resins were placed directly on the beam for scanning. Background was measured and subtracted.

Four explanted specimens, all Pinnacles, were cleaned of residual biological material by soaking 24 hours at room temperature in a sodium hypochlorite solution (7.85 % available chlorine), followed by rinsing extensively with water and drying in a vacuum oven at room temperature. It should be noted that ISO 12891, which describes recommended protocols for retrieval analysis of surgical implants including removal of biological tissue, does not list a protocol for cleaning

polypropylene, but it does recommend sodium hypochlorite for cleaning the closely related polyolefin, ultra-high molecular weight polyethylene.

Molecular Weight Comparisons / Gel Permeation Chromatography (GPC)

The high temperature GPC protocol used in our work closely follows that described in ASTM D6474-12, Standard Test Method for Determining Molecular Weight Distribution and Molecular Weight Averages of Polyolefins by High Temperature GPC. Solutions of the polypropylene meshes for GPC analysis were prepared by weighing out about 20 mg of the sample and adding sufficient 1,2,4-trichlorobenzene (TCB) to give a concentration of about 1.5 mg/ml. Solutions of the explanted polypropylene meshes were prepared by weighing out 5 to 19 mg of the sample (depending upon how much was available) and adding 8 to 13 ml of 1,2,4-trichlorobenzene (TCB) to give a concentration ranging from 0.55 to 1.55 mg/ml. Each sample was heated for approximately 4 hours at 160°C using a PL-SP 260 High Temperature Sample Preparation instrument. After 1 hour of heating, the samples were shaken for 30 minutes. After the four hours of heating, the samples were transferred to autosampler vials using a pipettor equipped with a 1 µm glass fiber filter.

The samples were analyzed using a Polymer Labs GPC-220 gel permeation chromatograph. The instrument was controlled by a Dell computer system and contained three detectors: Precision Detector PD2040 (static light scattering-two angles of 15° and 90°), Viscotek 220 Differential Viscometer, and a Polymer Labs differential refractometer. The analysis of the light scattering data was performed using Precision Detectors software. The triple detection analysis was done using Polymer Labs Cirrus software. The GPC-220 contained three PLGel Mixed B-LS 10µm

columns + a 10 μm guard column with TCB as the solvent at a flow rate of 1 ml/min at 145°C. The TCB contained 0.01% BHT (butylated hydroxytoluene) as a stabilizer.

Thermogravimetric Analysis (TGA)

TGA was performed using a Discovery Series TGA from TA Instruments. The runs involved a 10 °C per minute ramp from room temperature up to 600 °C under air (flow rate 25 ml/min). Sample masses used were typically about 3 mg. To observe the effect of anti-oxidant on thermo-oxidative stability, anti-oxidant was removed from a sample of Pinnacle mesh so that its thermal stability could be compared with that of Pinnacle with anti-oxidant present. The protocol for removing the antioxidant was as follows: The Pinnacle mesh was weighed out using the laboratory balance (about 0.2 g). It was placed in a vial with 12 mL of TCB as solvent. The solution was heated to 160 °C for one hour (no agitation),then agitated for 30 min still at 160 ° C and with no agitation kept at 160 °C for another hour. The hot PP solution was slowly poured into room temperature ethanol, which is a solvent for the anti-oxidant but a non-solvent for polypropylene. The precipitate was filtered using a Buchner funnel under vacuum with a 0.2 micron pore size PTFE filter. The filtered precipitate was re-dissolved in 10 mL of TCB at 160 °C for one hour and then agitated for 30 minutes still at 160 °C. The newly dissolved solution was treated as before to recover the PP.

Scanning Electron Microscopy (SEM) Testing

SEM was used to take highly magnified images of pelvic repair meshes. The sample preparation for the exemplar control samples consisted of removing the Pinnacle and Obtryx devices from their original packaging and cutting an approximately 1 cm^2 patch of mesh with fine laboratory shears and mounting this patch onto an approximately 1 cm diameter SEM sample holder, which

is a flat disk of aluminum. The samples were adhered to the aluminum holders with a double sided, electrically conductive tape made specifically for that purpose. The explanted samples were contained in jars of formalin solution. Previous published work has shown that preservation of explanted samples in formalin solution did not alter the structure and chemistry of the mesh fibers [8]. Explanted samples were rinsed in ultrapure (deionized) water and then allowed to air dry. After drying, the explanted samples were mounted on aluminum SEM sample holders with double sided, conductive tape.

Traditional SEM testing would require these samples to be coated with a very thin layer of gold, platinum or carbon to increase their electrical conductivity. This was not necessary and was not done in our testing because we employed the FEI Magellan 400, a state of the art SEM instrument in the W. M. Keck Electron Microscopy Center at the University of Massachusetts Amherst. SEM images were taken in secondary electron imaging mode using an Everhart-Thornley detector. Images were taken at 1 kV accelerating voltage and a beam current of 3.1 pA.

In the preparation for SEM testing sample XP-11 and only XP-11 was treated with sodium hypochlorite solution for the removal of biological tissue using the published procedure of Bracco [8], i.e. 6-14% active chlorine for 24 hours, followed by washing in pure water.

Energy Dispersive X-Ray Spectroscopy (EDS)

EDS testing is performed inside the SEM instrument on the same samples and at the same time as SEM imaging. The Magellan SEM was equipped with an Oxford Instruments X-MAX EDS detector. When the electrons used in the imaging process of the SEM interact with the sample material, X-rays are generated, which have energies specific to the types of atoms that compose the sample. EDS detects these X-ray energies and provides information about the atomic

composition of the sample [13,14]. Because EDS is performed in conjunction with SEM imaging, it is possible to select specific locations in the highly magnified image of the sample and then use EDS to obtain composition information at that precise location.

EDS was used to look for the presence of oxygen in polypropylene fibers, which would indicate that degradation due to oxidation has occurred. In the explanted samples, in which biological tissue is also present, EDS can be used to distinguish clean polypropylene fibers from biological tissue or fibers coated with biomaterial. We must base our conclusions related to fiber degradation on clean polypropylene fibers and make sure we are not looking at biological films coating the fibers. Polypropylene fibers damaged by oxidation and biological material contain both carbon and oxygen; however, only biological materials contain nitrogen. The presence or absence (or near absence) of nitrogen as detected by EDS is the key discriminator between clean polypropylene fibers from which valid conclusions can be drawn or biomaterial covered fiber from which conclusions are less straightforward. To obtain a good EDS signal we needed to increase SEM accelerating voltage to 3 kV and the beam current to 50 pA. This means that the images that accompany the EDS spectra show some charging (analogous to glare in optical photographs).

Results

Characterization of Non-Implanted Polypropylene Mesh, and Polypropylene resins:

SEM and EDS of Non-Implanted Mesh

The Pinnacle exemplar (non-implanted) mesh was observed from two locations: the central area (Pinnacle Control 1), and one of the branches (Pinnacle Control 2).

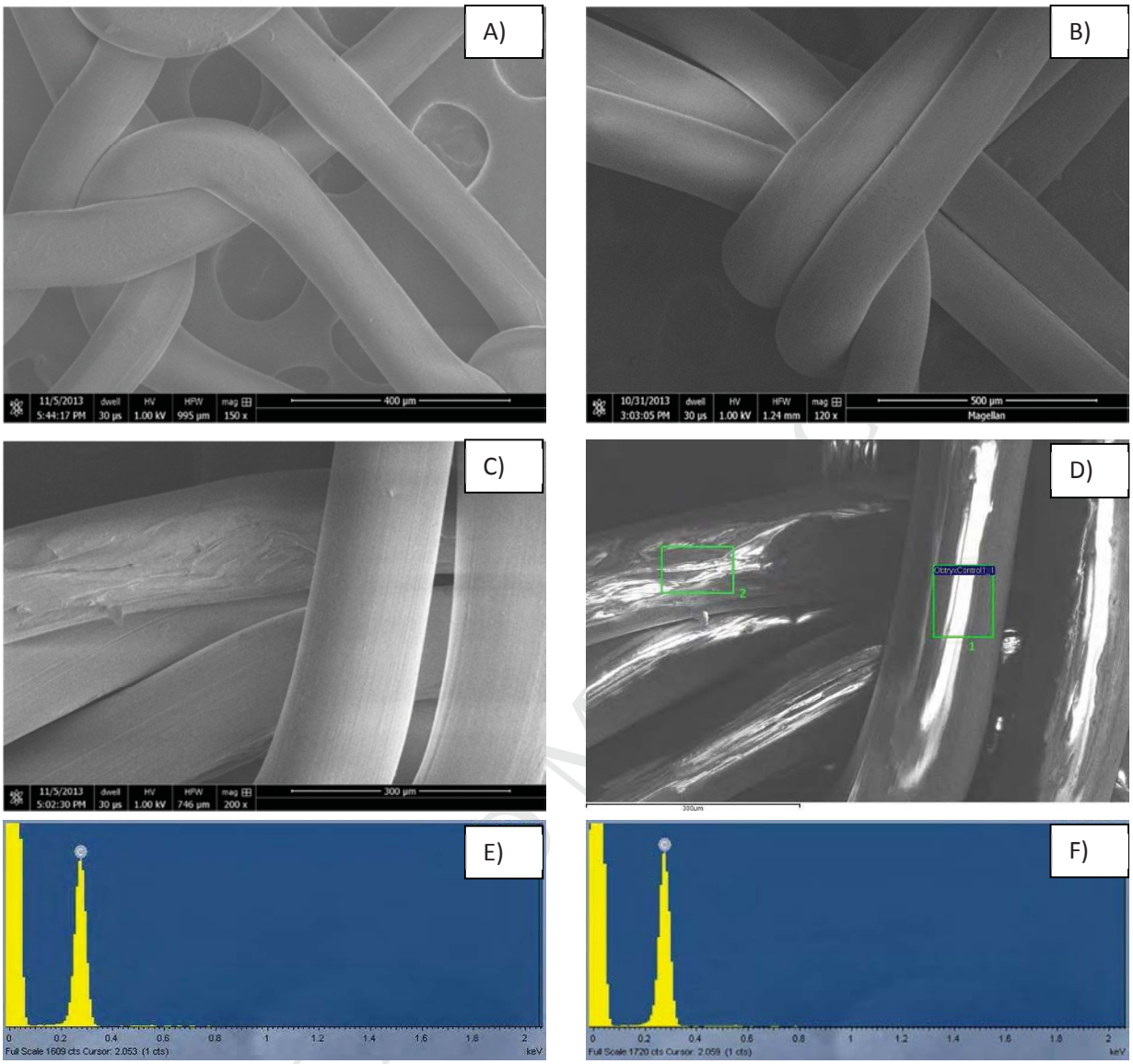

Figure 1 A) SEM image of Pinnacle Control 2. B) SEM image of Obtryx exemplar control. C) SEM image of Obtryx exemplar control showing abraded region. D) Locations for EDS Spectra. E) EDS Spectrum from region 1 in Figure 3b. F) EDS Spectrum from region 2 in Figure 3b.

Figure 1A shows a representative SEM image from Pinnacle Control 2. The fibers are clean and free of horizontal cracking. There are rough spots and minor abrasions on the fibers, which are not associated with oxidative degradation. The fibers also display faint striations along the length of the fibers. These striations are characteristic of the bare polypropylene fiber surface. EDS spectra on these PP fibers show only one spectroscopic peak, corresponding to carbon. Pure polypropylene is composed of only two elements - carbon and hydrogen, but hydrogen produces

no signal in EDS. Thus, these spectra are consistent with pure polypropylene, which has not undergone oxidative degradation. The results for Pinnacle Control 1 are similar to those for Pinnacle Control 2.

Figure 1B shows a representative SEM image from the Obtryx exemplar control. The fibers are clean and free of horizontal cracking, and display faint striations along the length of the fibers, characteristic of the bare polypropylene fiber surface. Figure 1C shows a region of the Obtryx control with an abraded region of fiber. Figure 1D shows an image of the same area as Figure 1C but taken at the higher beam current and higher accelerating voltage conditions used for EDS. There are two numbered, boxed regions overlaid on this image, one on smooth fiber and one on the abraded region. EDS spectra were recorded for the material inside each of these boxes and the results are shown in Figures 1E and 1F. Both of these regions show only a carbon peak, no oxygen is detected. The absence of oxygen in the abraded region of the fiber shows that this type of damage is not associated with oxidative degradation.

TEM of Non-Implanted Mesh

Figure S1 shows a TEM image of the internal structure of polypropylene fibers from the non-implanted Pinnacle control sample; the TEM method is described in the Supplementary Material. Results for the Obtryx control are the same as for Pinnacle. The darker regions of the sample are amorphous and are more susceptible to damage from oxidation than the lighter, crystalline regions. In order to obtain the light-dark contrast observed in this TEM image, the sample has been stained by exposure to ruthenium tetroxide (RuO_4) vapors [15-20]. This stain is an oxygen containing compound, which reacts with the polypropylene material by oxidation chemistry similar to the oxidation of polypropylene in air or in the body [17]. The difference, however, is that the oxidizing stain carries along ruthenium metal that gets deposited at the site of oxidation

and shows up as dark in the TEM imaging. Thus the amorphous regions of the internal fiber structure are dark in the TEM image precisely because they are more susceptible to oxidation. The dappled texture of this TEM image is consistent with the presence of crystalline and amorphous regions. The size scale of the dark and light patches in this TEM image is approximately 10 nm, consistent with what is known about polyolefin semicrystalline morphology [15].

FTIR of Non-Implanted Mesh

The FTIR spectra of non-implanted Pinnacle and Obtryx are given in Figures 2A and 2B. For all

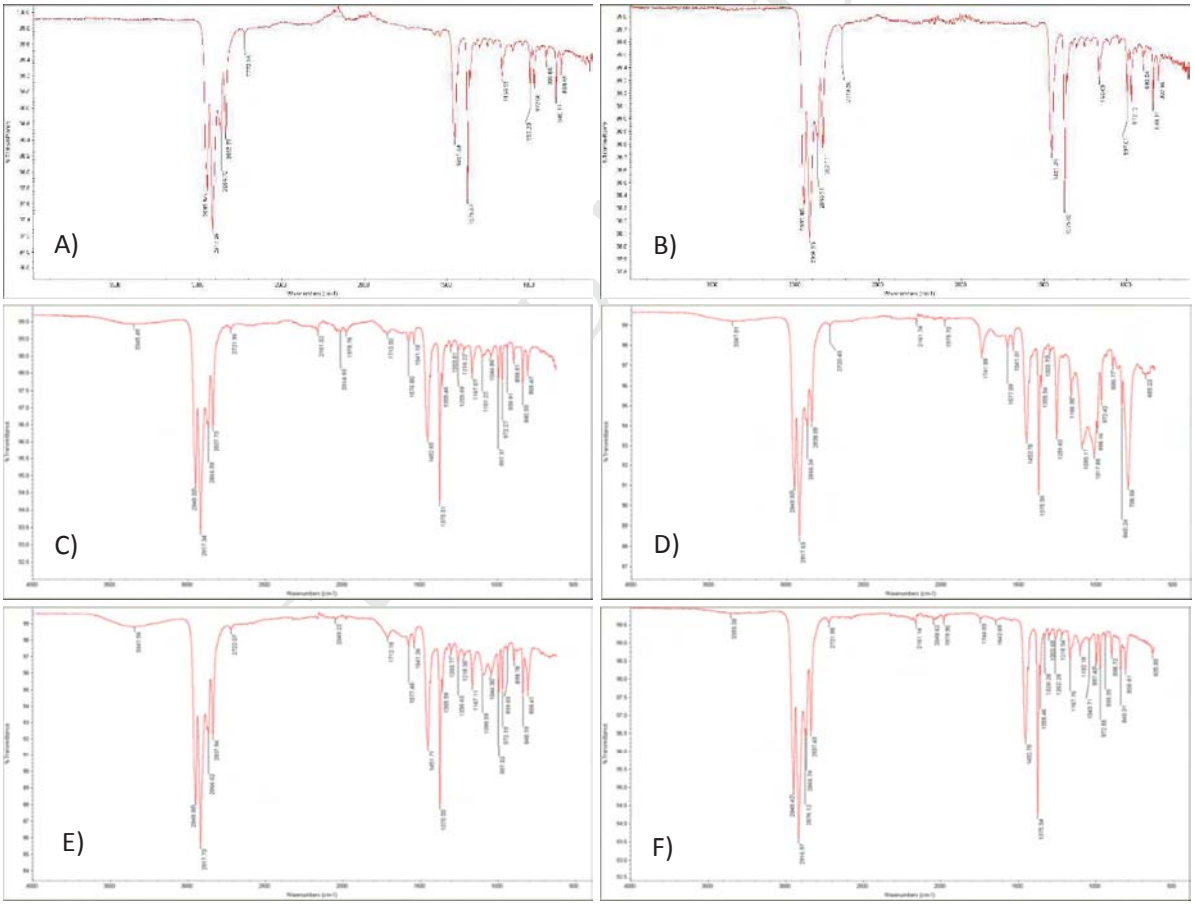

Figure 2: A) FTIR of Pinnacle control. B) FTIR of Obtryx control. C) FTIR spectrum of XP-8 explant. D) FTIR spectrum of XP-3 explant. E) FTIR spectrum of XP-10 explant. F) FTIR spectrum of XP-7 explant.

seven polypropylene mesh samples the FTIR spectra are nearly identical to each other (see

Supplementary Data, Figures S2-S6) and to those of the four commercial isotactic polypropylene (Figures S7-S10) and show the absorption peaks expected for polypropylene (alkyl C-H stretching peaks between about 2850 and 2960 cm^{-1} and at 1450 and 1375 cm^{-1}). There is no evidence of oxidation in these materials, which would be seen by a broad absorption peak centered around 3400 cm^{-1} for hydroxyl and hydroperoxide groups and peaks between about 1700 and 1750 cm^{-1} corresponding to ketones, aldehydes, and carboxylic acids.

To confirm that bleach cleaning of the explants did not cause oxidation of the specimens, we also carried out FTIR analysis of bleach treated non-implanted Pinnacle (Figure S11). Consistent with published literature (8) and the known chemical compatibility of polypropylene, no evidence of oxidation is seen and the spectrum is essentially identical to the spectrum obtained for non-implanted Pinnacle prior to the bleach treatment.

GPC of Non-Implanted Mesh

GPC was used to characterize the average molecular weights and polydispersities of the polypropylene comprising the various non-implanted polypropylene meshes. The GPC chromatograms, obtained in triplicate for the various meshes using differential refractometry (DRI), a 15 degree light scattering detector, a 90 degree light scattering detector, and a viscosity detector, are shown in Figures S12-S39. The high level of reproducibility of the GPC data obtained with the various detectors can be seen in these figures. The elution behavior of all seven of the polypropylene mesh exemplar materials is very similar, as seen in Figures S40-S43, where the 2nd runs of each are compared. The very similar nature of the chromatograms show that the polypropylene molecules that make up these seven meshes are very similar in their molecular weight characteristics.

A comparison of calculated weight-average (M_w) and z-average (M_z) molecular weights and polydispersity indices (M_w/M_n) of the seven mesh materials is shown in Table 1.

Table 1. Average molecular weights and polydispersity indices for polypropylene meshes*

PP Mesh	**M_z x 10^{-5}**	**M_w x 10^{-5}**	**M_w/M_n**
Advantage	10.2	3.87	3.90
Lynx	10.1	3.72	4.28
Obtryx	10.0	3.85	4.06
Pinnacle	11.3	3.98	5.58
Prefyx	11.1	3.91	4.32
Solyx	10.9	3.98	4.42
Uphold	9.53	3.77	3.96

* Averages from triplicate runs using triple detection (DRI, light scattering, viscometer).

M_z and M_w values for all the resins are identical within experimental error. Number-average molecular weights for six of the seven samples are also identical within experimental error with only Pinnacle showing a lower value (outside one standard deviation and just within two standard deviations from the mean for the seven samples). These small differences could reflect different lots of Marlex polypropylene being used in their manufacture or variations in the processing conditions.

TGA of Non-Implanted Mesh

Commercial polypropylene resins almost always contain antioxidants to retard the well-known thermo-oxidative degradation of polypropylene [4]. In order to determine whether or not the polypropylene used to make the various meshes contain antioxidants, we compared their degradation behavior in air using TGA to that of four commercial polypropylene resins, which all contain various proprietary stabilizer packages. The TGA results, obtained in triplicate for the four commercial polypropylenes, Exxon Achieve 6936G1, Exxon PP3155, Metocene 500 MFR, and Metocene MF6504, are shown in Figures S44 – S47, respectively. It can be seen from these triplicate runs that, while the TGA results are highly reproducible for a particular sample in terms of the temperature at which degradation begins, they do show some run-to-run variability. This likely reflects the fact that the dispersion of anti-oxidant in the polymer is not completely homogeneous, resulting in some variations in anti-oxidant content for the extremely small samples analyzed in TGA – typically about 3 mg.

Triplicate TGA runs of the seven polypropylene meshes are shown in Figures S48 – S54. As with the commercial polypropylene resins, there is some run to run variability in these experiments, but overall the degradation profiles for each sample are quite reproducible. An overlay of the first TGA runs for all eleven polypropylenes (commercial resins and meshes) is shown in Figure 3A.

From Figure 3A it is clear that the thermo-oxidative degradation behavior of six of the seven polypropylene meshes are very similar to that of three of the four commercial polypropylene resins. Lynx shows slightly better thermal stability than the other mesh samples, which is surprising since all seven meshes are made from the same Marlex polypropylene. This could, again, reflect lot to lot variations in Marlex or a change in the stabilizer package. Exxon PP3155 is more stable than all the other polypropylene materials likely reflecting a different stabilizer package or increased concentration(s) of stabilizer(s).

To show the effect of anti-oxidant on the degradation of PP, we compare the degradation behavior of Pinnacle mesh with that of Pinnacle with the anti-oxidant removed (as described above). Figure S55 shows triplicate TGA runs of Pinnacle without stabilizer, and Figure 3B compares the TGA behavior of Pinnacle with and with anti-oxidant. It can be seen in Figure S55 that a small amount of mass loss occurs on heating from room temperature to 150 °C. This is due to the loss of a small amount of residual TCB solvent that was used during anti-oxidant removal process and which was not completely eliminated by overnight vacuum drying at room temperature. Thermo-oxidative degradation begins at about 200 °C and is quite reproducible in

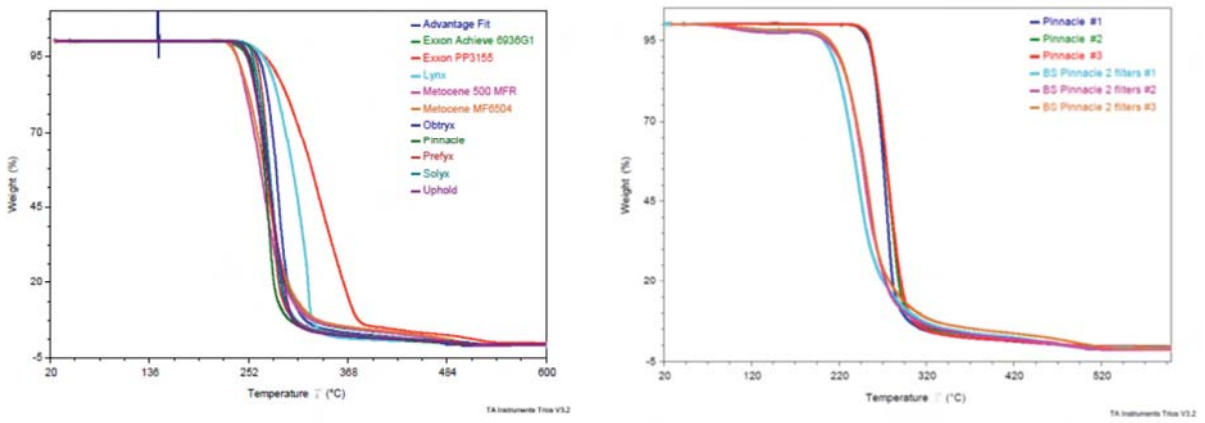

Figure 3: A) TGA overlay of all polypropylene samples. B) Thermal comparison on the effect of antioxidant on the stability of Pinnacle polypropylene.

the three runs.

The difference in thermo-oxidative stability between Pinnacle PP with and without anti-oxidant is clearly seen in Figure 3B. The *Pinnacle 2 Filters* samples are those where the anti-oxidant was removed, and the data are the same as in Figure S55. The three Pinnacle runs represent the actual Pinnacle mesh as received with anti-oxidant present, and the data are the same as in Figure S51. Whereas the PP samples without anti-oxidant start to thermo-oxidatively degrade at about 200 °C, the Pinnacle with anti-oxidant starts to degrade only at higher temperature (about 240 °C). The effect of antioxidant is also to shift the entire thermo-oxidative degradation process to higher temperatures. Note that polypropylene always undergoes thermo-oxidative degradation in these experiments; the effect of antioxidant is only to delay the process. Likewise, the degradation of polypropylene exposed to an oxidative environment, such as the human body, can be delayed but not prevented through use of antioxidants.

Characterization of Explanted Polypropylene Mesh:

SEM and EDS Results

SEM imaging of explanted PP-mesh samples showed various degrees of cracking transverse to the fiber axis. We have defined a numerical scale to quantify the degree of visible transverse cracking of the polypropylene fibers: 0 (no cracking); 1 (a few small cracks); 2 (numerous small

cracks); 3 (significant cracking); 4 (severe cracking); 5 (very severe cracking). Examples of these different levels of damage are shown in the SEM images of Figure 4.

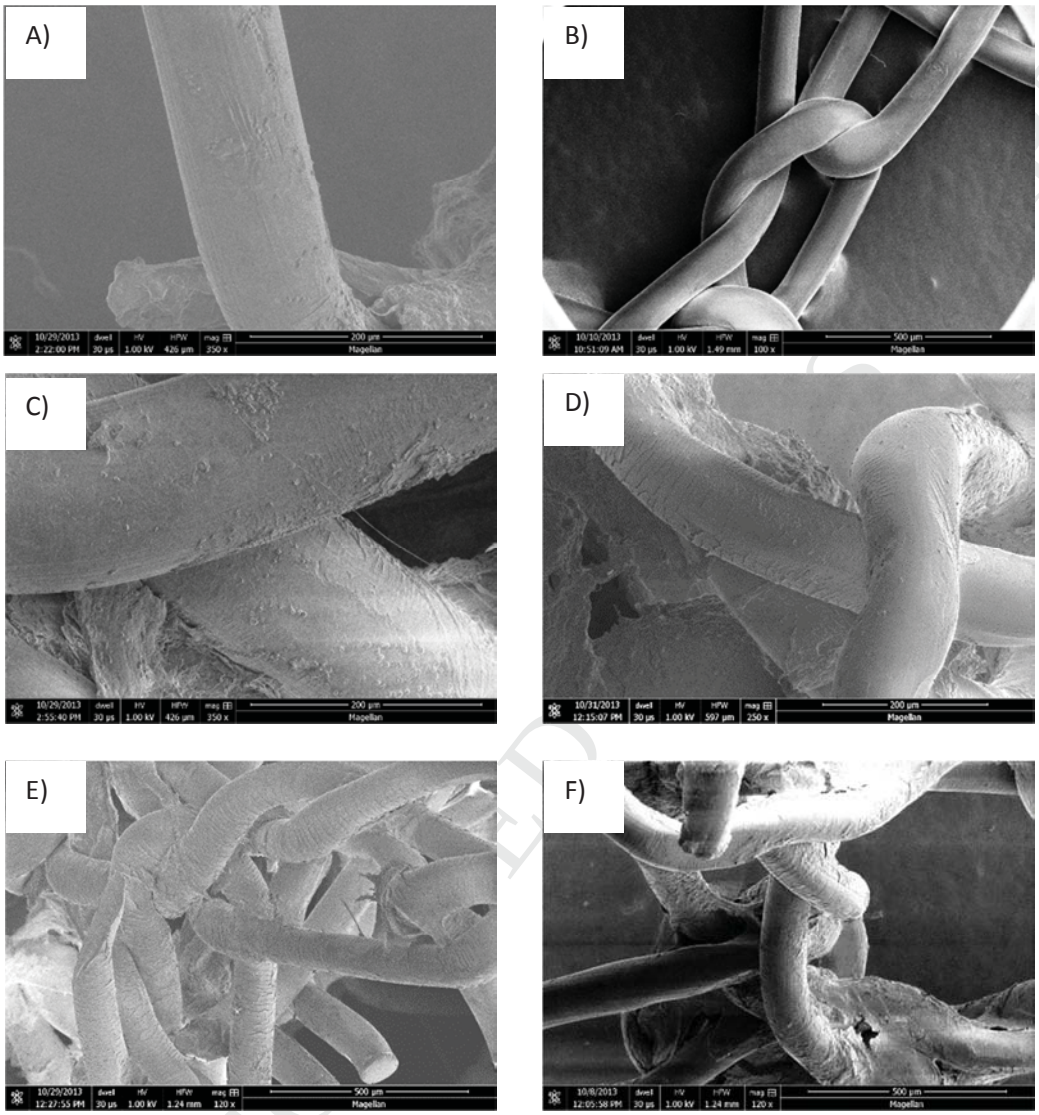

Figure 4: A) SEM image of polypropylene mesh fibers with a cracking level 0 (no cracking). [Pinnacle Control 1]. B) SEM image of polypropylene mesh fiber with cracking level 1 (a few small cracks) Cracks are visible near base of fiber in image. [XP-5]. C) SEM image of polypropylene mesh fiber with cracking level 2 (numerous small cracks) [XP-1]. D) SEM image of polypropylene mesh fiber with cracking level 3 (significant cracking) [XP-4]. E) SEM image of polypropylene mesh fiber with cracking level 4 (severe cracking) [XP-7]. F) SEM image of polypropylene mesh fiber with cracking level 5 (very severe cracking) [XP-8]

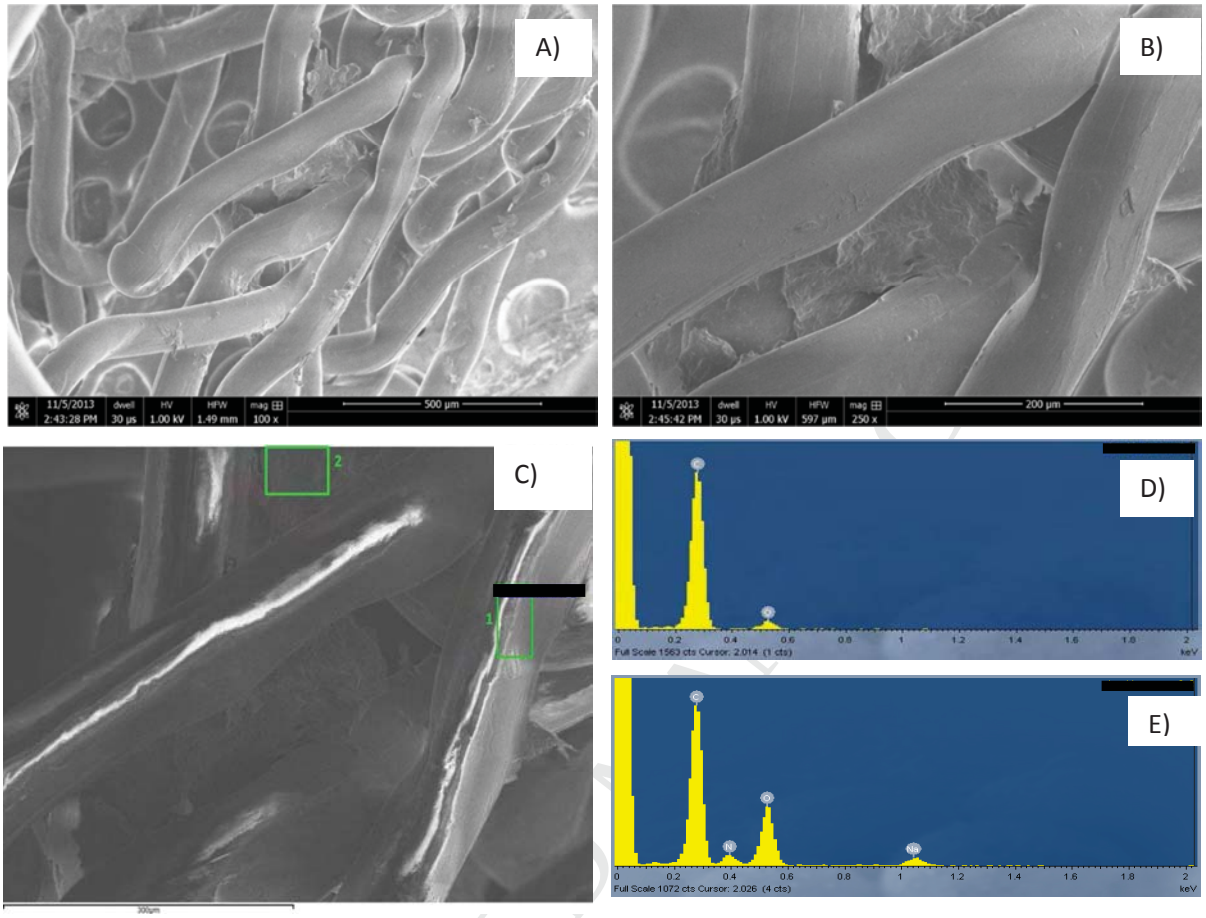

Figure 5: A) SEM of explanted Pinnacle Mesh fibers [XP-3]. B) SEM of explanted Pinnacle Mesh fibers [XP-3]. C) SEM image with regions selected for EDS. D) EDS Spectra from region 1 in Figure 5C. E) EDS Spectra from region 2 in Figure 5C

3.4.3.4 XP-3: Short Time Explant Pinnacle, Cracking Level 0:

Figure 5 shows representative SEM images of a Pinnacle mesh which was explanted after 1 year and 7 months. The fibers are mostly clean of biological material and no horizontal cracking is evident. Figure 5B is a higher magnification view of a section of the field of view of Figure 5A.

Figure 5C shows an image of the same region as Figure 5B taken under conditions for EDS. Figure 5D and 5E show the EDS spectra taken from boxed Regions 1 and 2. Region 1 on the clean fiber shows peaks for carbon and oxygen indicating polypropylene that been damaged by oxidation. Region 2 yields a spectrum with significant nitrogen as well as sodium, another

element associated with biological material, but not with polypropylene. These findings demonstrate that we are able to locate clean fiber in this sample and that oxidation of these fibers has occurred even before horizontal cracks appear. We are able to use a combination of SEM imaging and EDS to clearly distinguish between PP-fiber and biological material.

3.4.3.8 XP-7: Intermediate Time Explant Pinnacle, Cracking Level 4:

Figure 6 shows representative SEM images of a Pinnacle mesh explanted after 3 years and 3 months. Fibers were found that were largely clean of biological material and displayed severe

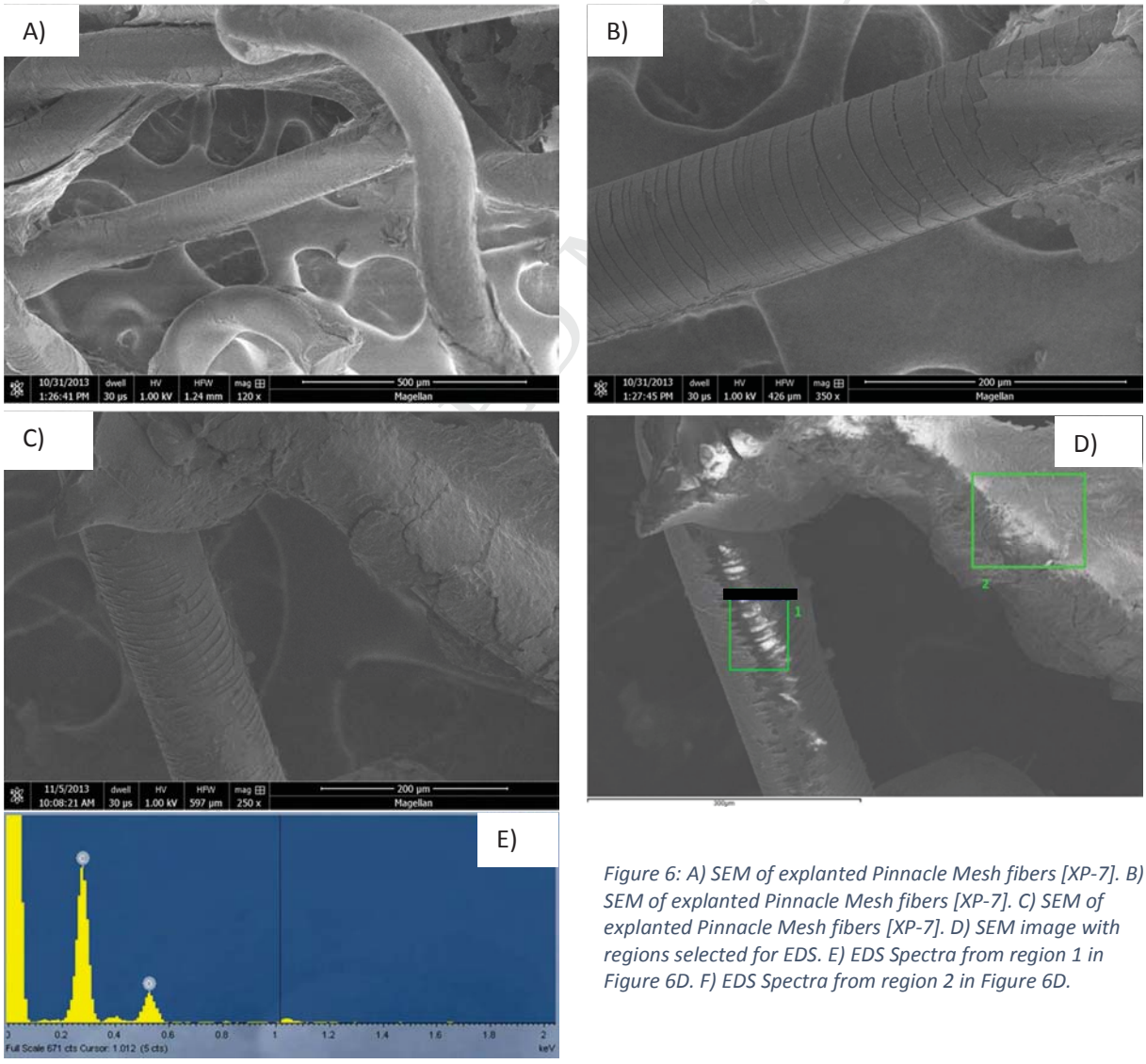

Figure 6: A) SEM of explanted Pinnacle Mesh fibers [XP-7]. B) SEM of explanted Pinnacle Mesh fibers [XP-7]. C) SEM of explanted Pinnacle Mesh fibers [XP-7]. D) SEM image with regions selected for EDS. E) EDS Spectra from region 1 in Figure 6D. F) EDS Spectra from region 2 in Figure 6D.

horizontal cracking. In Figure 6C, the fiber on the left is clean of biological material while the fiber on the right is encrusted with biological material.

Figure 6D shows an image of the same region as Figure 6C taken under conditions for EDS. Figure 6E and 6F show the EDS spectra taken from boxed Regions 1 and 2. Region 1 on the clean fiber shows peaks for carbon and oxygen indicating polypropylene that been damaged by oxidation. A trace of nitrogen is also present indicating that a very small amount of biological material may be present, but not enough to obscure the polypropylene fiber surface. Region 2, on the biomaterial coated fiber, yields a spectrum with significant nitrogen and sodium consistent with biological material. These findings show that we are able to locate clean fiber in this sample and that oxidation of these fibers has occurred and is accompanied by severe horizontal cracking.

3.4.3.11 XP-10: Long Time Explant Pinnacle, Cracking Level 3:

Figure 7 shows representative SEM images of a Pinnacle mesh explanted after 4 years and 5 months. Fibers were found that were largely clean of biological material and displayed significant horizontal cracking.

Figure 7D shows an image of the same region as Figure 7C taken under conditions for EDS. Figure 7E and 7F show the EDS spectra taken from boxed Regions 1 and 2. Region 1 on the clean fiber shows peaks for carbon and oxygen indicating polypropylene that been damaged by oxidation. There is a trace amount of nitrogen present indicating the presence of some biological material but not enough to obscure the view of the horizontally cracked polypropylene surface. Region 2 yields a spectrum with significant nitrogen as well as some sodium, consistent with the presence of biological material.

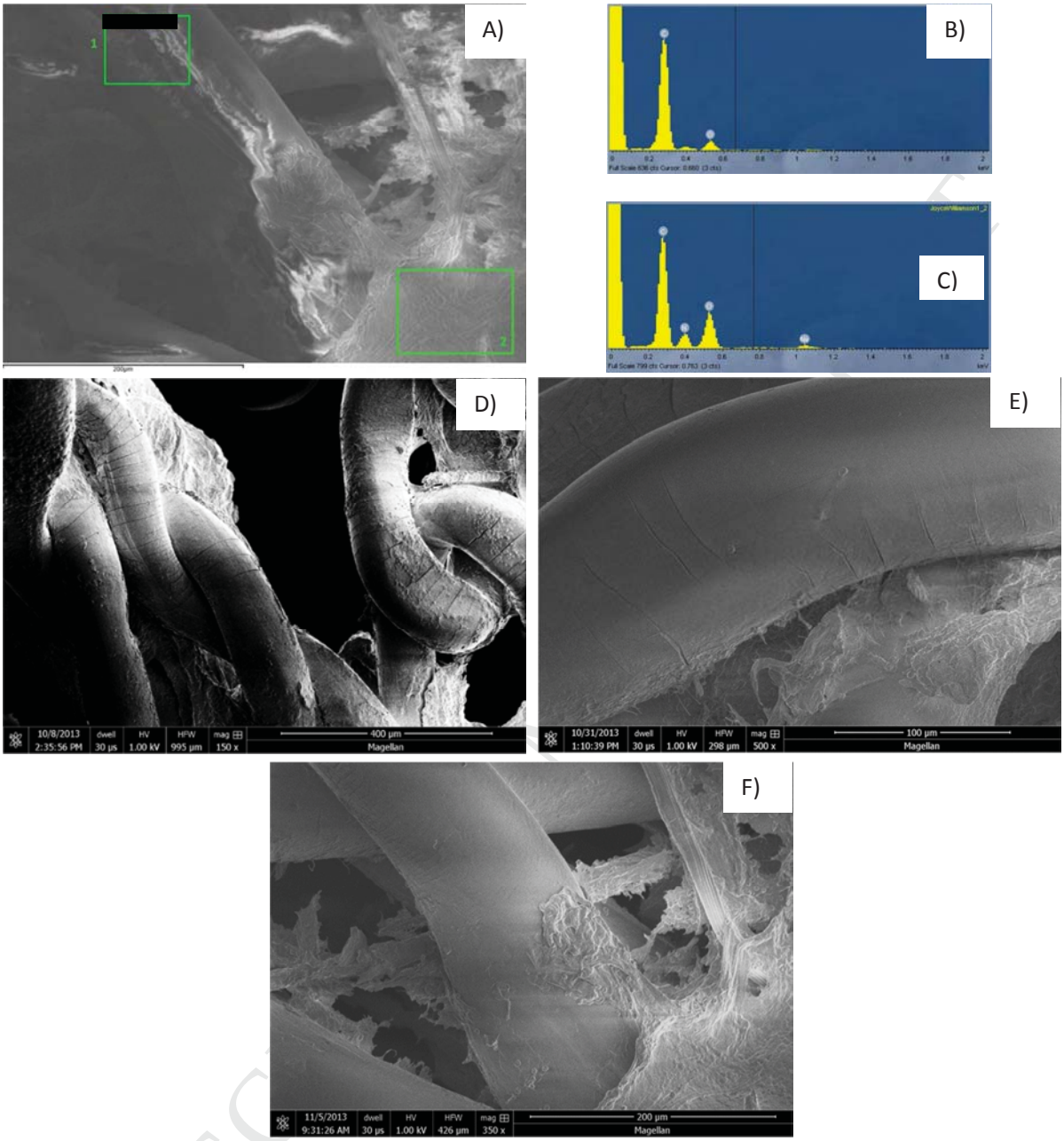

Figure 7: A) SEM image with regions selected for EDS. B) EDS Spectra from region 1 in Figure 13A. C) EDS Spectra from region 2 in Figure 13A. D) SEM of explanted Pinnacle Mesh fibers [XP-10]. E) SEM of explanted Pinnacle Mesh fibers [XP-10]. F) SEM of explanted Pinnacle Mesh fibers [XP-10].

The complete SEM and EDS data for all 11 explanted samples are given in the supplementary material (S56 – S111).

Four explanted specimens, all Pinnacles, were cleaned of residual biological material by soaking 24 hours at room temperature in a sodium hypochlorite solution and drying in a vacuum oven at

room temperature. Their FTIR spectra are given in Figure 2B-F. All four explants (DW-8, JL-3, JW-10, and SC-7) are Pinnacles. Clear signs of oxidation are seen in the FTIR spectra of all four implants as evidenced by broad peaks centered around 3400 cm^{-1} (hydroxyl and peroxide) and between 1700 and 1750 cm^{-1} (carbonyl). These data are consistent with the study of Liebert et al. [5], who detected both hydroxyls and carbonyl in their infrared studies of polypropylene filaments explanted from hamsters after various periods of time.

The GPC chromatograms, obtained in triplicate for sample XP-3 using differential refractometry, a 15 degree light scattering detector, a 90 degree light scattering detector, and a viscosity detector, are shown in Figure S112-S115 in blue and compared with the corresponding GPC traces (in red) of non-implanted Pinnacle (Pinnacle was also run in triplicate but only a single trace is shown in these figures because of their high reproducibility and to avoid clutter in the figures).

The high level of reproducibility of the triplicate runs is evident from the blue curves. It is apparent from all the chromatograms that the highest molecular weight components present in the non-implanted Pinnacle (those appearing at the smallest retention time) are lost upon implantation. The loss of the highest molecular weight components upon implantation is especially apparent with the light scattering and viscosity detectors, which are more sensitive to the higher molecular weight components in the sample. Preferential degradation of the highest molecular weight polymer chains is expected for a random degradation process; since higher molecular weight chains contain more bonds they are more likely to be broken. The loss of high molecular weight components may be quantified by comparing the weight-average molecular weights, Mw, and z-average molecular weights, Mz, for the two materials. Using a triple detector analysis, which takes into account results from RI, LS, and viscosity detectors, the non-

implanted Pinnacle has Mz = 1,151,000 and Mw = 388,000 while the XP-3 explanted sample has Mz = 648,000 and Mw = 291,000. In addition, the breadth of the molecular weight distribution is decreased for the XP-3 sample as compared to the non-implanted Pinnacle (Mw/Mn = 5.97 (Mn is number-average molecular weight) for Pinnacle as compared to Mw/Mn = 3.44 for XP-3. This is also indicative of a chain scission process occurring during implantation; chain scission by "visbreaking" is commonly used in the polypropylene industry to reduce the breadth of the molecular weight distribution by selectively breaking longer chains [21]. Any random chain degradation process will eventually yield a most probable molecular weight distribution characterized by Mw/Mn = 2 [22].

The three other Pinnacle explants of adequate quantity for GPC analysis were also analyzed by SEC and the results are presented in the Supplementary Materials (S116-S127). These materials also showed clear evidence of chain scission: reduced Mz and Mw and narrowing of the polydispersity upon implantation.

Discussion

FTIR, SEM and EDS testing shows that the Pinnacle and Obtryx non-implanted control meshes reveal no signs of degradation and contain no oxygen, or only trace amounts, as one would expect from the chemical structure of pure polypropylene, which contains no oxygen bearing chemical functionality.

All the explanted samples, spanning the range from short to long implant times, show the presence of oxygen in the polypropylene fibers indicating that oxidation chemistry has occurred. FTIR shows peaks resulting from hydroxyl and hydroperoxide groups and from ketone,

aldehyde, and carboxylic acids. All of these chemical functionalities are oxygen containing products formed by the oxidative degradation of polypropylene. The oxidative degradation of polypropylene is also known to cleave polymer chains which reduces molecular weight and narrows the polydispersity of the molecular weight distribution. GPC testing shows reductions in z-average (Mz) and weight average (Mw) molecular weights and a narrowing in polydispersity (Mw/Mn) for the four explant samples tested. These included both Obtryx and Pinnacle meshes and included short intermediate and implantation times.

EDS also shows the presence of oxygen in all the explanted mesh samples. This oxidative degradation of explanted fibers is accompanies by cracking transverse to the fiber axis as observed by SEM. The cracking looks similar to that observed in previous SEM studies of degraded, explanted PP fibers from hernia and pelvic meshes produced by a number of manufacturers [8-11]. Our results show that cracking generally becomes progressively more severe with increasing length of implantation. Two out of four short time explants show no visible cracking of the fibers, but EDS indicates that oxidative degradation has already started to occur. Clearly, significant oxidation damage occurs in the fibers before the first cracks become visible.

These results are summarized in Table 2 and in Figure8.

Table 2: Summary of Testing Results

SAMPLE	LENGTH OF TIME IMPLANTED	IMPLANT TIME CLASSIFICATION	MODEL	Cracking Observed by SEM	Oxidation in Fibers Observed by EDS	Oxidation In Fibers Observed by FTIR	Mz from GPC	Mw from GPC	Mw/Mn from GPC
Obtryx Control	—	None		0	no	no	1,030,000	377,000	4.26
Pinnacle Control 1	—	None		0	trace amounts	no	1,151,000	388,000	5.97
Pinnacle Control 2	—	None		0	no*	not tested			
XP-1	1 YR, 4 MOS.	Short	Obtryx Halo	2	yes	not tested			
XP-2	1 YR, 6.5 MOS.	Short	Pinnacle	0	yes	not tested			
XP-3	1 YR, 7 MOS.	Short	pinnacle	0	yes	yes	648,000	291,000	3.44
XP-4	1 YR, 10 MOS.	Short	Pinnacle	3	yes	not tested			
XP-5	2 YRS, 2.5 MOS.	Intermediate	Pinnacle	1	yes	not tested			
XP-6	2 YRS, 11 MOS.	Intermediate	Pinnacle	0	yes	not tested			
XP-7	3 YRS, 3 MOS.	Intermediate	Pinnacle	4	yes	yes	847,000	344,000	3.95
XP-8	4 YRS, 1 MO.	Long	Pinnacle	5	not tested	yes	735,000	326,000	3.53
XP-9	4 YRS, 4 MOS.	Long	Pinnacle	4	yes	not tested			
XP-10	4 YRS, 5 MOS.	Long	Pinnacle	3	yes	yes	742,000	314,000	3.91
XP-11	4 YRS, 9 MOS.	Long	Obtryx Halo	5	yes	not tested			

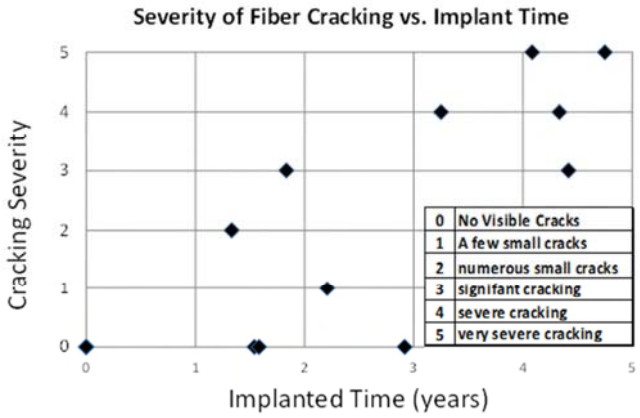

Figure 8. Cracking severity as a function of implanted time.

Collectively, the testing results provide a consistent picture of polypropylene mesh fibers, which become oxidized upon implantation into the human body. This oxidation produces oxygen containing chemical functionalities that are detected by FTIR and EDS. All explanted samples show the presence of oxygen either by EDS, FTIR, or a combination of the two. Oxidative degradation of the polypropylene results in a decrease in polypropylene molecular weight, which is known to reduce the strength of the fibers and can eventually lead to fiber failure. The degradation of the structure of the fibers due to oxidation and reduction in molecular weight eventually results in the appearance of horizontal cracking on the fiber surfaces, which becomes more severe at longer implantation times. This cracking is consistent with weakening of the

implanted fibers. This overall picture of oxidative degradation of implanted PP fibers is consistent with previous studies on explanted PP fibers using the same and similar analytical techniques, as reviewed above.

Based on experiments in which degraded explant PP fibers were only extracted with hexane (i.e. no bleach treatment to remove biological material), Bracco [8] postulated that the primary cause of the cracked and degraded morphology of the PP fibers was their absorption of small organic molecules of biological origin including cholesterol, squalene, and esterified fatty acids. Subsequent researchers (Clave [11]; Lefranc [12]) have mentioned Bracco's small organic molecule hypothesis but have generally attributed degradation of the explanted PP fibers primarily to oxidation. It is our opinion that Bracco has shown that some small, biologically derived organic molecules can be absorbed into the outer layers of implanted PP fibers. His study has not shown, however, that this process is the direct cause of fiber degradation, although it very well could be a contributing factor that aids oxidation. In the last paragraph of the *Discussion* section of their paper Bracco et al. [8] try to explain their idea as to how absorption of small organic molecules could contribute to fiber degradation. The phenomenon that they are trying to explain is well known to polymer scientists and is referred to as plasticization [23,24]. Plasticizers are small organic molecules that are absorbed into a solid polymer and soften it. The mechanism of this softening involves increasing the free volume space in amorphous regions of a solid polymer structure. The amorphous regions of the PP semicrystalline structure are susceptible to plasticization by absorption of the types of biological, small organic molecules that Bracco observed. In particular esterified fatty acids are well known to plasticize polymers [25-27]. It is likely that an increase in free volume of the amorphous regions of implanted PP fibers due to plasticization from the absorption of small, biological organic molecules facilitates

increased penetration into the PP fibers by oxygen and other oxidizing chemical species, thus accelerating PP fiber degradation due to oxidation.

Conclusions

The overall degradation process of PP pelvic meshes may be summarized as follows. The implant causes increased activity by oxidative enzymes in the vicinity of the implant. This leads to an oxidative degradation process that is evidenced by appearance of hydroxyl and then carbonyl groups in the polypropylene, as observed by infrared spectra. There is accompanying degradation of the polypropylene molecular weight, and this process may be delayed, but not prevented, by the presence of antioxidants in the polypropylene. Antioxidants are preferentially consumed by the oxidizing species and finally the concentration falls below a level required to protect the polymer and oxidative degradation occurs [28]. This degradation is accompanied by a decrease in mechanical properties (embrittlement, loss of mass, decreased melting temperature, reduced compliance) of the polypropylene [9, 28]. In particular, the surface and amorphous regions of the polypropylene are selectively degraded, resulting initially in cracks and, on longer exposure, fragmentation of the implant. In Figures S102 and S103 the fact that the cracks actually penetrate into the body of the fiber is very evident. If a crack penetrates an entire fiber, then by definition the fiber is broken. Our SEM images (Figures 4E&F, S74, S87, S91) show broken fiber ends in conjunction with surface cracking. Cracks, such as those visible in Figure S103, result in a stress concentration and thus weaken the fiber, resulting in a tendency for cracks to deepen and fibers to fail. Costello (Reference 10) discusses PP fiber fragmentation as a result of implantation.

Acknowledgements

This study was initially conducted in litigation and sponsored by claimants against Boston Scientific Corporation.

References

1) Usher, FC, Ochsner, J, Tuttle, LL. Use of Marlex mesh in the repair of incisional hernias. American Surgery 24: 969-974 (1958).

2) Ratner B, Hoffman AS, Schoen FJ, Lemons JE. Biomaterials Science. Academic Press, 1996.

3) Williams DF. Biodegradation of surgical polymers. J Mater Sci, 17:1233-1246 (1982).

4) Vasile C. Degradation and Decomposition. Handbook of Polyolefins, 2nd edition, 2000. Ch. 17.

5) Liebert TC, Chartoff RP, Cosgrove SL, McCluskey RS. Subcutaneous Implants of Polypropylene. J Biomed Mater Res 10, 939-951 (1976).

6) Usher FC, Ochsner J, Tuttle LL. Use of Marlex mesh in the repair of incisional hernias. American Surgery 24, 969-974 (1958).

7) Costa L, Luda MP, Trossarelli L, Brach del Prever EM, Crova M, Gallinaro P. In vivo UHMWPE biodegradation of retrieved prosthesis. Biomaterials 19, 1371-1385 (1998).

8) Bracco P, Brunella V, Trossarelli L, Coda A, Botto-Micca F. Comparison of polypropylene and polyethylene terephthalate (Dacron) meshes for abdominal wall hernia repair: A chemical and morphological study. Hernia 9, 51–55 (2005).

9) Costello CR, Bachman SL, Ramshaw BJ, Grant SA. Materials Characterization of Explanted Polypropylene Hernia Meshes. J Biomed Mater Res Part B: Appl Biomat 83, 44-49 (2007).

10) Costello CR, Bachman SL, Grant SA, Cleveland DS, Loy TS, Ramshaw BJ. Characterization of Heavyweight and Lightweight Polypropylene Prosthetic Mesh Explants from a Single Patient. Surgical Innovation 14, 168-176 (2007).

11) Clave A, Yahi H, Hammon J-C, Montanari S, Gounon P, Clave H. Polypropylene as a Reinforcement in Pelvic Surgery is Not Inert: Comparative Analysis of 100 Explants. Int. Urogynecol J 21, 261-270 (2010).

12) Olivier Lefranc, Yves Bayon, Suzelei Montanari, Philippe Gravagna, and Michel Thérin. Reinforcement Materials in Soft Tissue Repair: Key Parameters Controlling Tolerance and Performance – Current and Future Trends in Mesh Development, New Techniques in Genital Prolapse Surgery (2011). DOI: 10.1007/978-1-84882-136-1_25

13) J. I. Goldstein, D. E. Newbury, P. Echlin, D. C. Joy, A. D. Romig Jr., C. E. Lyman, C. Fiori, E. Lifshin. Scanning Electron Microscopy and X-ray Microanalysis: A Text for Biologists, Materials Scientists, and Geologists 2nd Edition. Chapters 5-9.

14) M. J. Dykstra Biological Electron Microscopy: Theory, Techniques, and Troubleshooting 236 (1992).

15) J. X. Li, W. L. Cheung RuO4 Staining and Lamellar Structure of α- and β-PP J. Appl. Polym. Sci. 72, 1529–1538 (1999).

16) G. M. Brown and J. H. Butler, New method for the characterization of domain morphology of polymer blends using ruthenium tetroxide staining and low voltage scanning electron microscopy (LVSEM) Polymer. 38, 3937-3945 (1997).

17) John S. Trent, Jerry I. Scheinbeim, and Peter R. Couchman Ruthenium Tetraoxide Staining of Polymers for Electron Microscopy Macromolecules 16, 589-598 (1983).

18) Hong, S.; Bushelman, A.A.; MacKnight, W.J.; Gido, S.P.; Lohse, D.J.; Fetters, L.J. Morphology of semicrystalline block copolymers: polyethylene-b-atactic-polypropylene. Polymer 42, 5909-5914 (2001).

19) J.H. Lee, M.L. Ruegg, N.P. Balsara,* Y. Zhu, S.P. Gido, R. Krishnamoorti, M. Kim, Phase Behavior of Highly Immiscible Polymer Blends Stabilized by Balanced Surfactants, Macromolecules 36, 6537-6548 (2003).

20) Shujun Chen, Souvik Nandi, H. Henning Winter, and Samuel P. Gido, Oriented lamellar structure and pore formation mechanism in CSX-processed porous high-density polyethylene Macromolecules 39, 2849-2855 (2006).

21) Grein C. Toughness of Neat, Rubber Modified and Filled and Nucleated Polypropylene: From Fundamentals to Applications. In Intrinsic Mobility and Toughness of Polymers II, Adv. Polym. Sci. 188, 43-104 (2005).

22) Flory PJ. Principles of Polymer Chemistry, Cornell University Press, Ithaca, 1953, p. 321.

23) I. M. Ward. Mechanical Properties of Solid Polymers 2nd Edition. (New York: John Wiley and Sons, 1983) p.174.

24) J. J. Aklonis and W. J. MacKnight. Introduction to Polymer Viscoelasticity 2nd Edition. (New York: John Wiley and Sons, 1983) pp. 64-65.

25) Frank P. Greenspan , Ralph J. Gall. Epoxy Fatty Acid Ester Plasticizers. Ind. Eng. Chem., 45, 2722–2726 (1953).

26) Frank P. Greenspan , Ralph J. Gall. "Epoxy Fatty Acid Ester Plasticizers. Preparation and Properties" J. Am. Oil Chem. Soc. 33, 391-394 (1956).

27) E. M. Sadek, A. M. Motawie, A. M. Hassan, E. A. Gad. "Synthesis and evaluation of some fatty esters as plasticizers and fungicides for poly(vinyl acetate) emulsion" Journal of Chemical Technology and Biotechnology 63(2), 160–164 (1995).

28) Vasile C. Degradation and Decomposition. In Vasile C, editor. Handbook of Polyolefins, 2nd edition, New York: Marcel Dekker, 2000. Ch. 20.

In Vivo Oxidative Degradation of Polypropylene Pelvic Mesh

Adam Imel[1], Thomas Malmgren[1], Mark Dadmun[1], Samuel Gido[2,*], Jimmy Mays[1,*]

[1]Department of Chemistry, University of Tennessee, Knoxville, TN 37996

[2]Department of Polymer Science and Engineering, University of Massachusetts, Amherst, MA 01003

*Corresponding authors: Samuel Gido, email gido@mail.pse.umass.edu, fax 413 545 0082; Jimmy Mays, email jimmymays@utk.edu, fax 865 974 9304

Supplementary Data

In this document the TEM method employed is described and the TEM image obtained for non-implanted Pinnacle after staining with ruthenium is presented.

FT-IR spectra of non-implanted Advantage, Lynx, Prefyx, Solyx, and Uphold exemplars and of four commercial polypropylene resins, Exxon Achieve 6936G1, Exxon PP3155, Metocene 500 MFR, and Metocene MF6504, are then presented. The FT-IR spectrum of non-implanted Pinnacle after bleach treatment, used in cleaning explanted samples is then shown to demonstrate that the fibers are not oxidized by the bleach treatment.

GPC chromatograms, obtained in triplicate for the various non-implanted polypropylenes, are then presented based on four different types of detection. The high level of reproducibility of the GPC curves demonstrate the reproducibility of the techniques employed for their analysis.

TGA curves for the various polypropylene resins are then presented in order to compare their thermos-oxidative stability. Small run to run variations in TGA are observed due to the very small sample sizes employed.

Additional SEM images and EDS spectra, not included in the body of the paper due to space limitations are presented. Finally, multi-detector GPC data for explanted polypropylene fibers are presented. These data, again run in triplicate, show the reproducibility of the GPC method employed. They are compared to the SEC chromatogram of the non-implanted polypropylene (Pinnacle) to demonstrate visually that high molecular weight polypropylene chains are degraded upon implantation.

Transmission Electron Microscopy (TEM)

Samples for TEM are ultrathin sections cut from the interior of the polypropylene mesh fibers of the Pinnacle and Obtryx exemplar controls. Approximately 50 to 70 nm thick sections were cut transverse to the fiber axis with a Leica Ultracut Cryoultramicrotome using a Diatome diamond knife and operated at -100 ºC. The polypropylene fibers were not embedded for microtoming. Instead, single fibers were attached to the tip of an aluminum pin, microtoming sample holder with histoprep tissue freezing medium. This water soluble material is solid at cryogenic temperatures and anchors the fiber during microtoming. After the microtomed sections are collected on 600 mesh copper TEM sample grids, the grids are floated on the surface of deionized water. This dissolves any adhered histoprep leaving only polypropylene fiber sections on the grids.

The samples were stained by exposing the grids holding the samples to the vapors of an aqueous solution of RuO_4 for 1 hour and 20 minutes. This staining agent reacts preferentially with the portions of the polypropylene fiber material, which are most susceptible to oxidation [1-3]. As it

does, this reagent deposits ruthenium (Ru) metal atoms in those regions of the sample marking them and making them appear darker relative to unstained material in TEM imaging.

TEM imaging was performed at an accelerating voltage of 200 kV in a JEOL 2000 FX-II instrument equipped with a LaB_6 filament. The results are shown in Figure S 1.

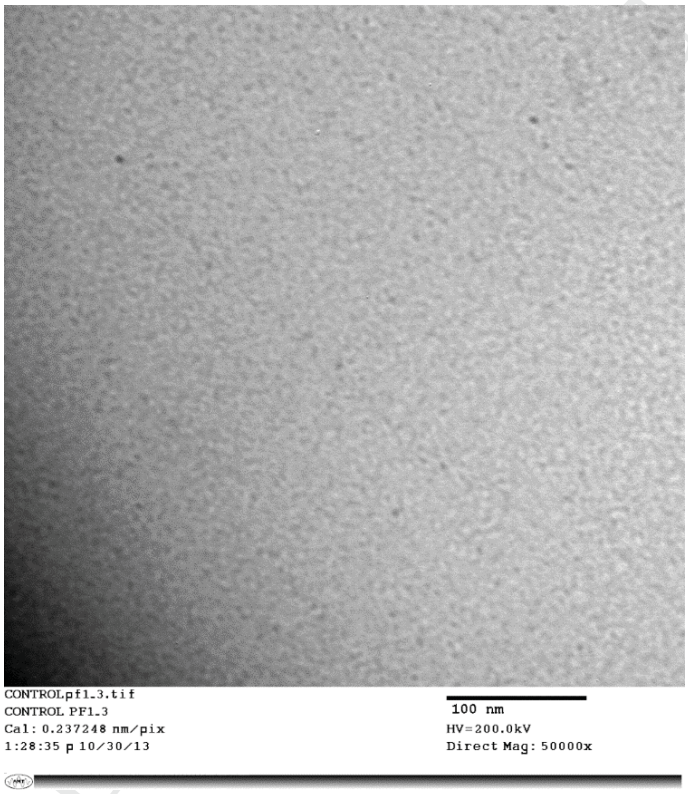

Figure S 1: TEM image of internal polypropylene fiber structure (Pinnacle Control 1).

FTIR spectra of non-implanted Advantage, Lynx, Prefyx, Solyx, and Uphold exemplars are shown in Figures S 2 – S 6, respectively.

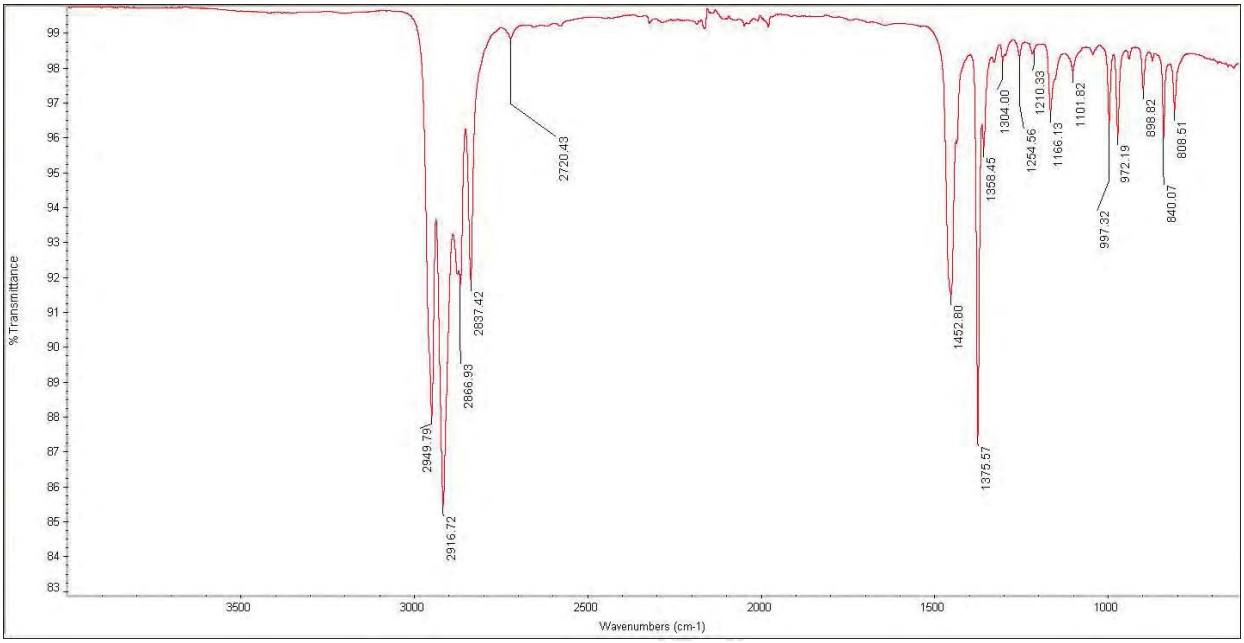

Figure S 2: FTIR spectrum of Advantage polypropylene mesh.

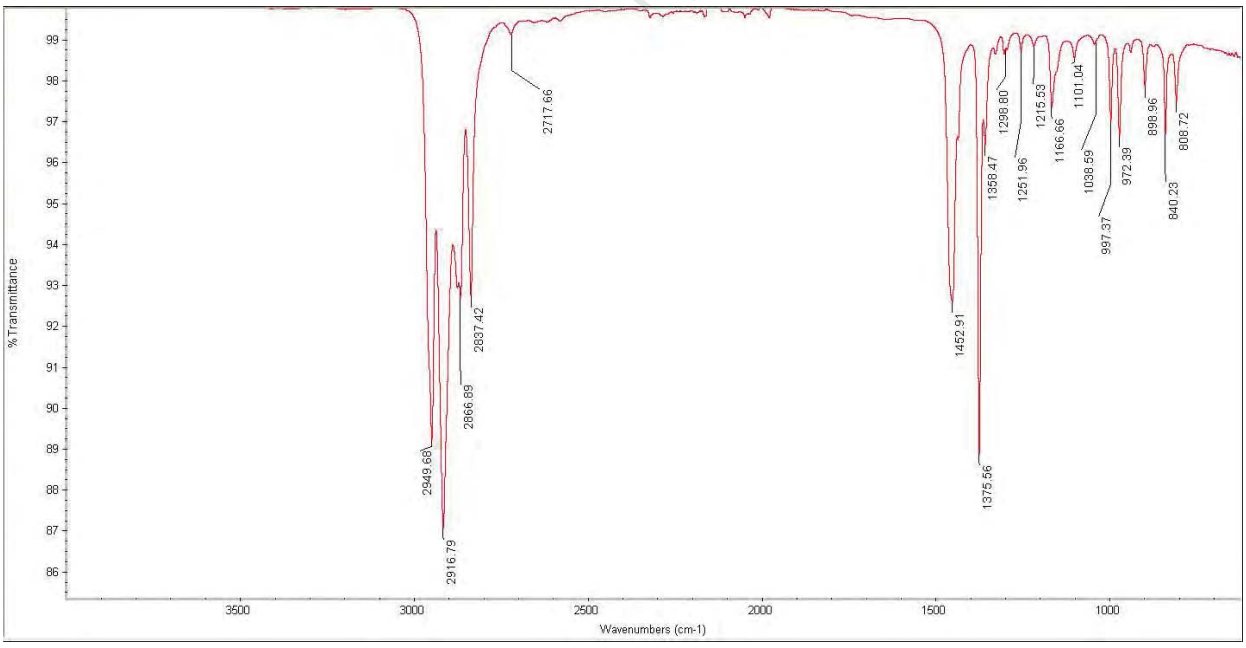

Figure S 3: FTIR spectrum of Lynx polypropylene mesh.

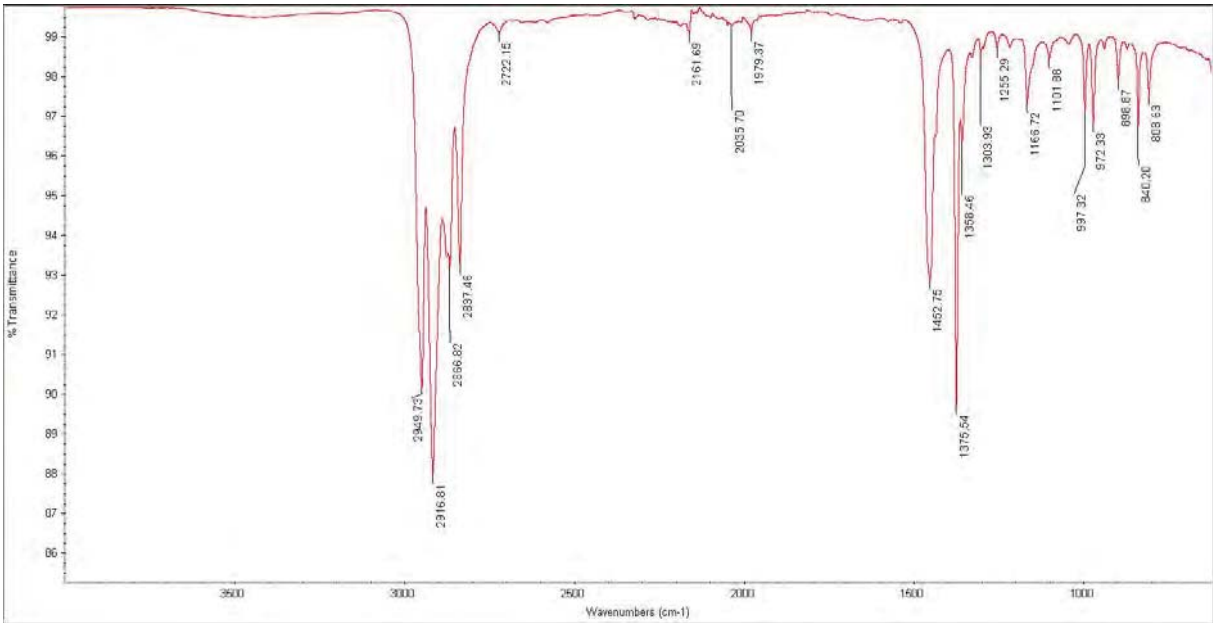

Figure S 2: FTIR spectrum of Prefyx polypropylene mesh.

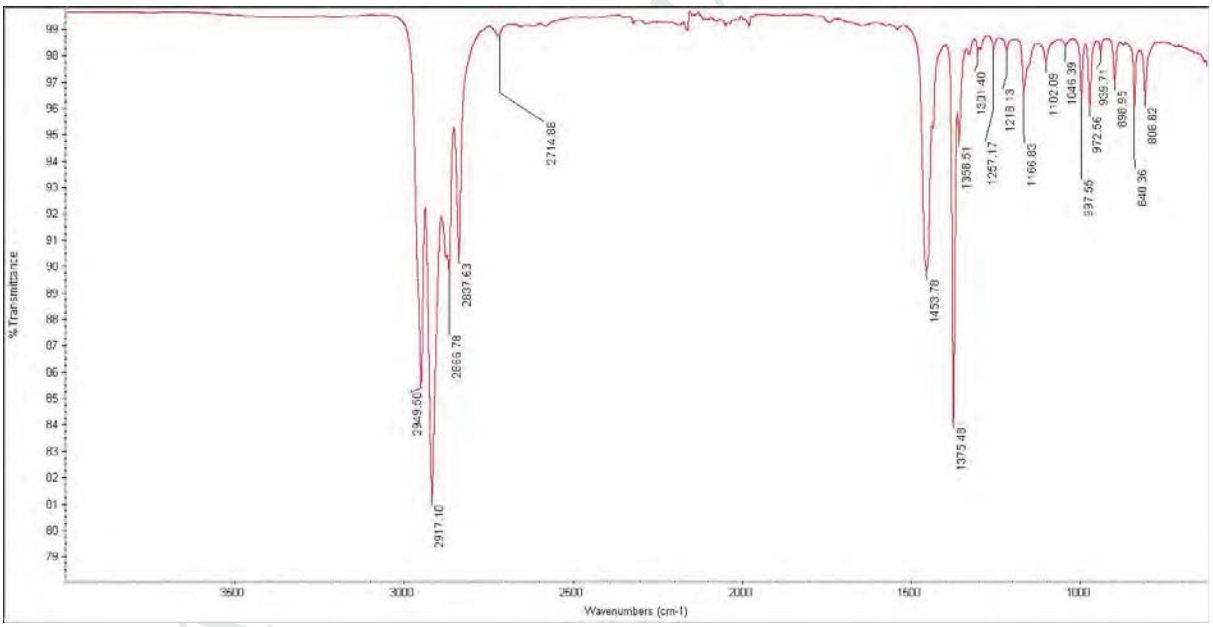

Figure S 3: FTIR spectrum of Solyx polypropylene mesh.

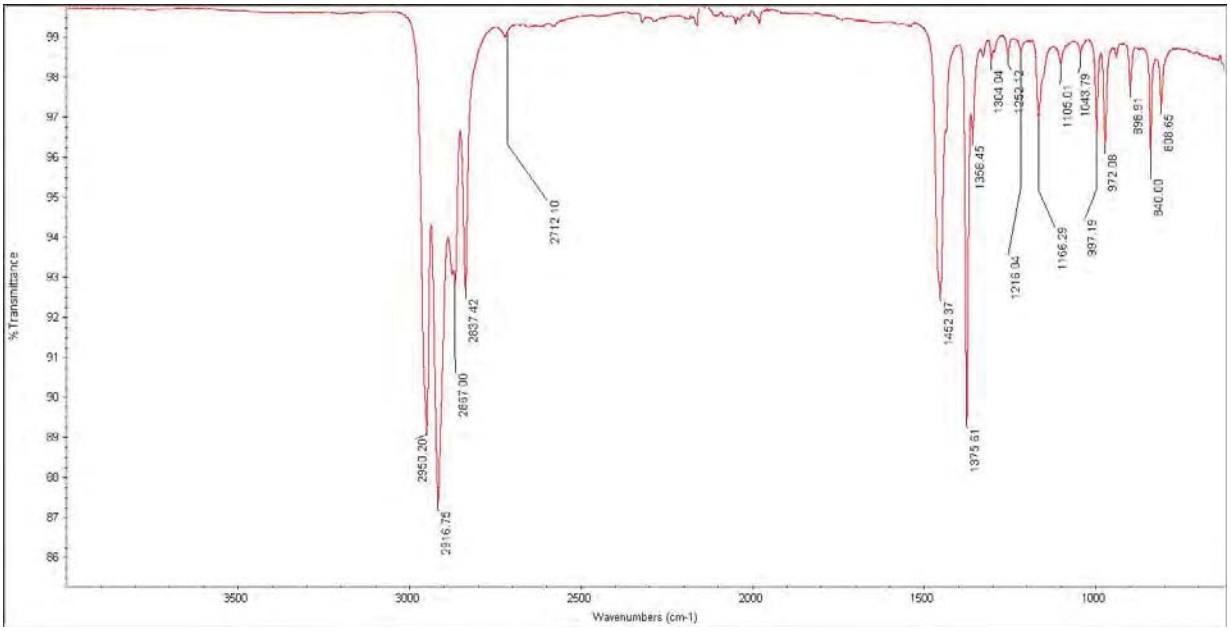

Figure S 4: FTIR spectrum of Uphold polypropylene mesh.

The FTIR spectra for the four commercial polypropylene resins, Exxon Achieve 6936G1, Exxon PP3155, Metocene 500 MFR, and Metocene MF6504, are shown in Figures S 7-S 10, respectively.

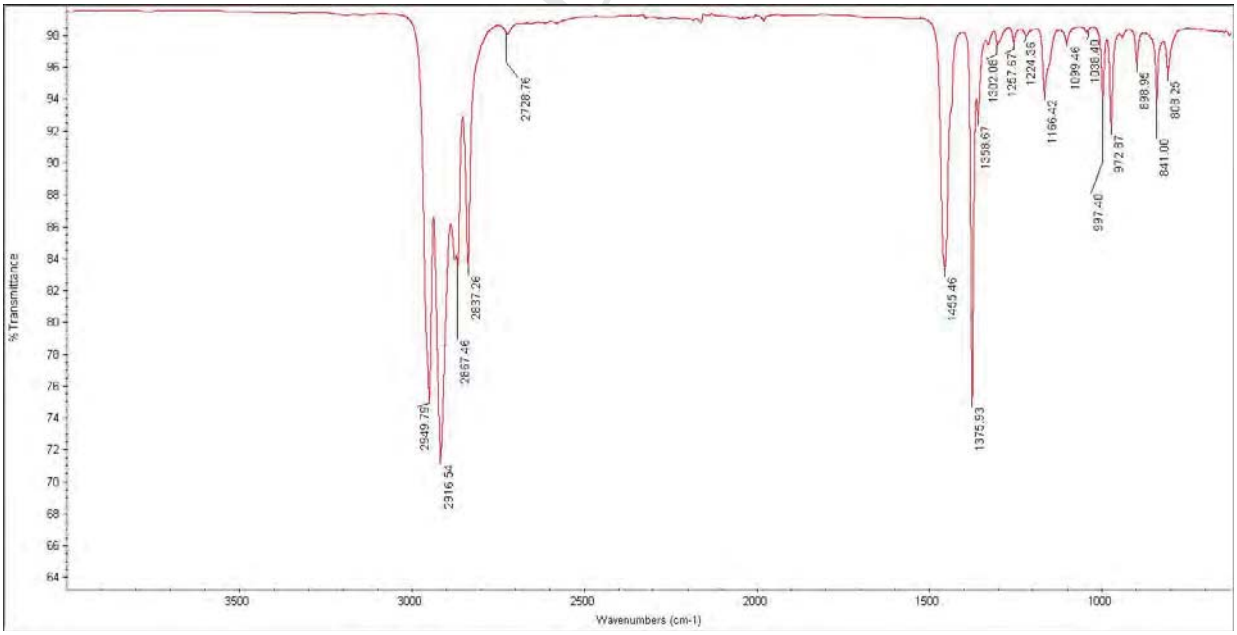

Figure S 5: FTIR spectrum of Exxon Achieve 6936G1 polypropylene.

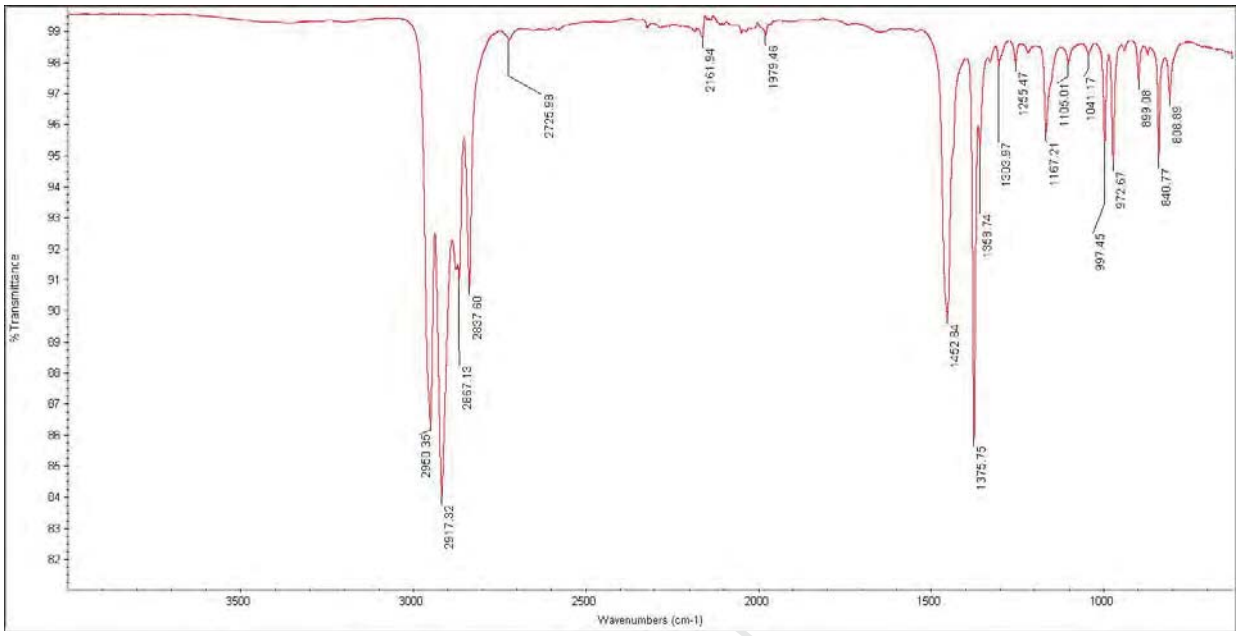

Figure S 6: FTIR spectrum of Exxon PP3155 polypropylene.

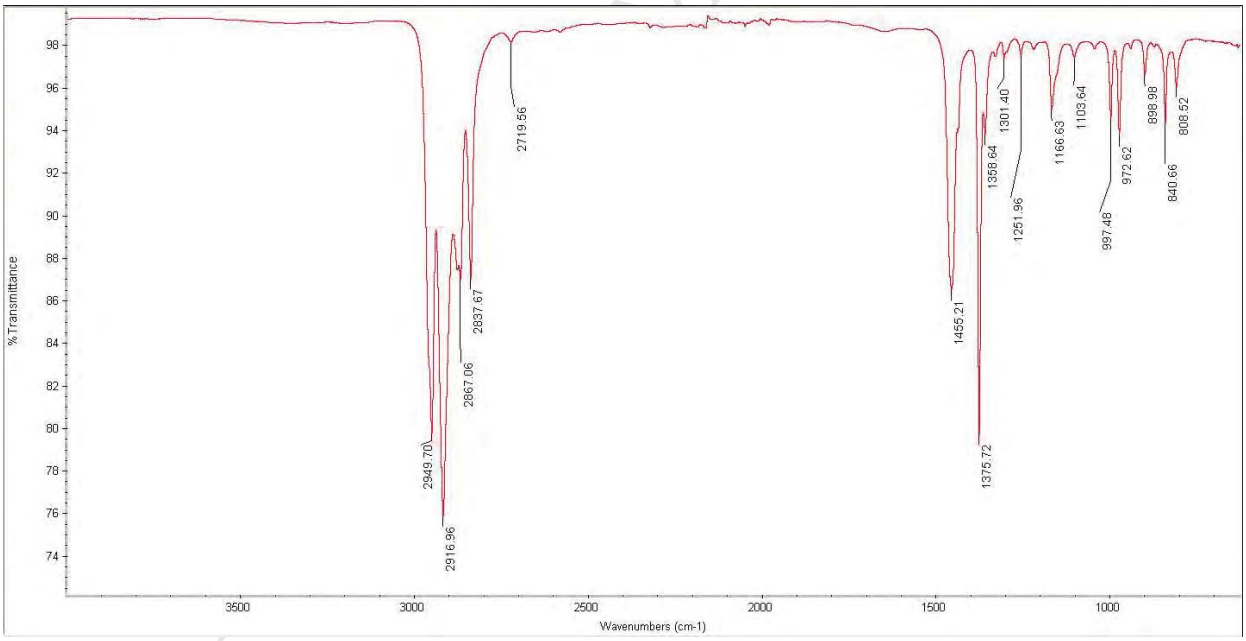

Figure S7: FTIR spectrum of Metocene 500 MFR polypropylene.

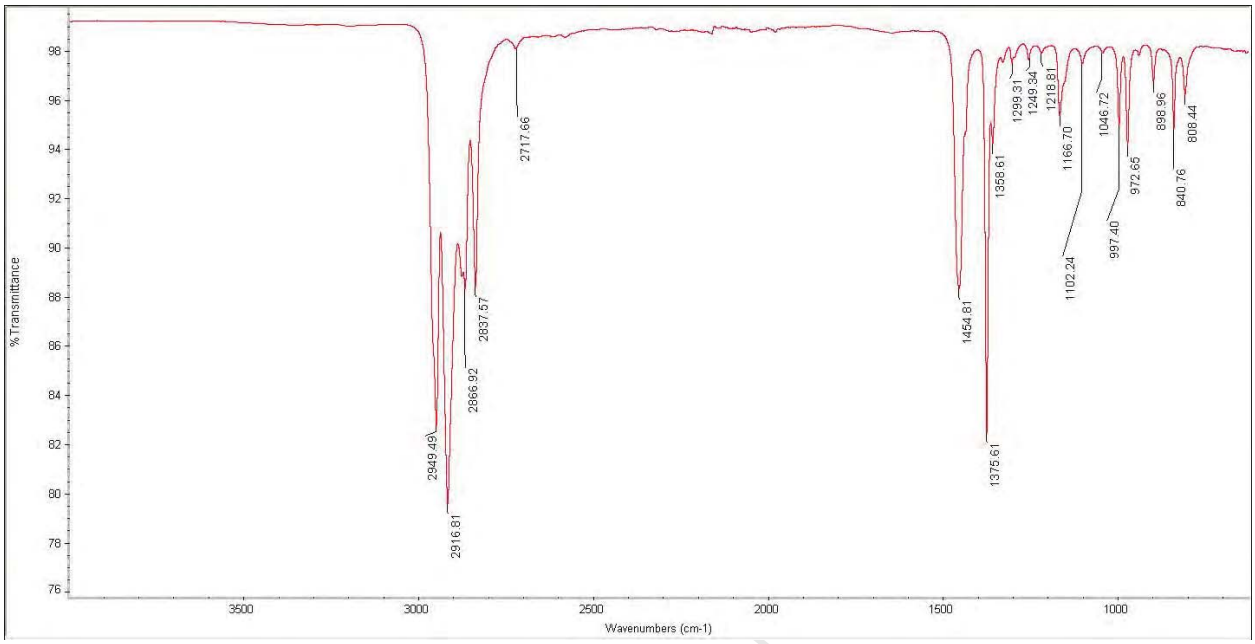

Figure S 8: FTIR spectrum of Metocene MF6504 polypropylene.

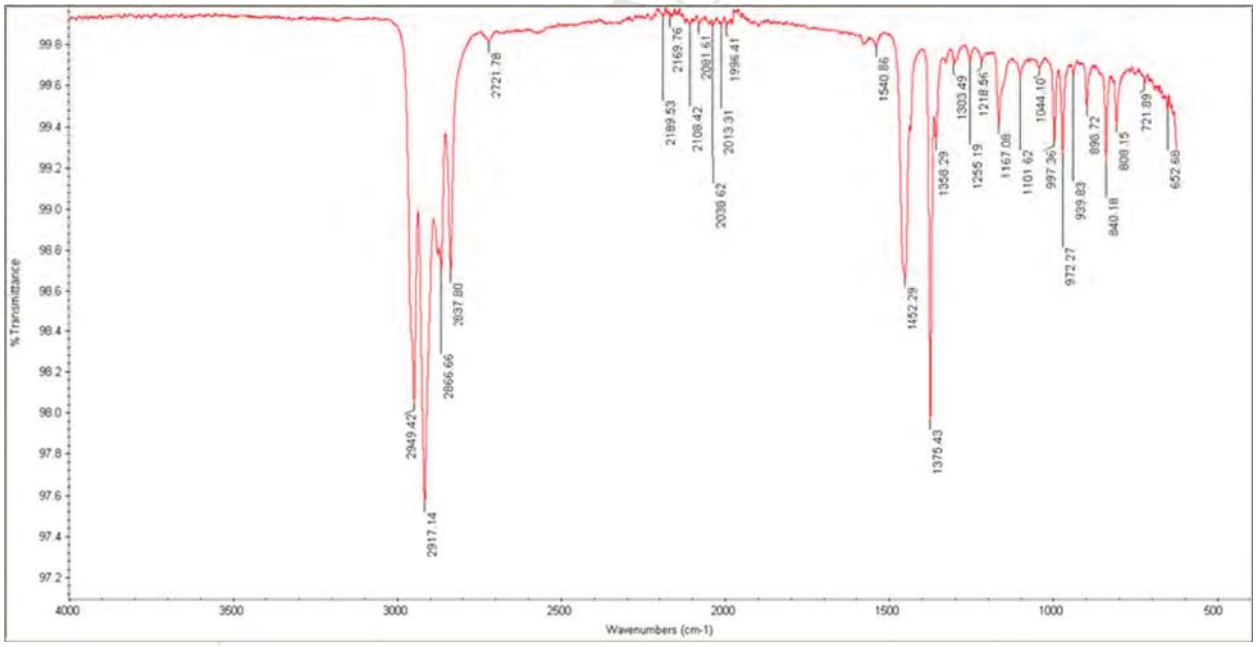

Figure S 9: FTIR spectrum of non-implanted Pinnacle after bleach treatment.

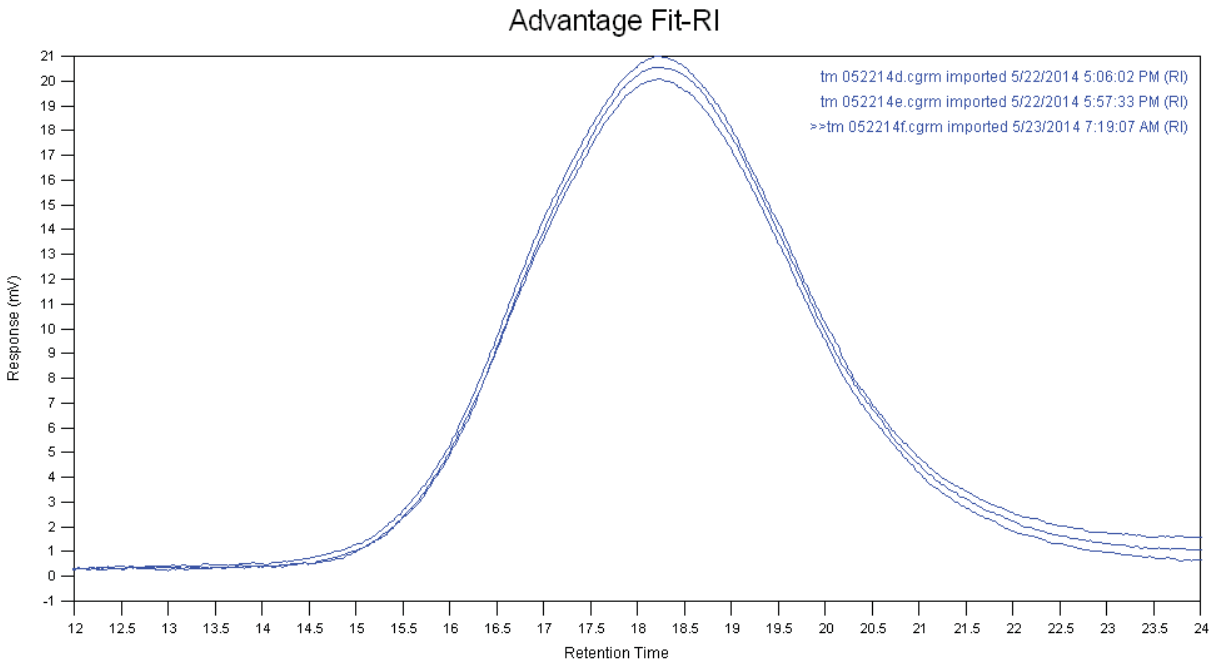

Figure S 112: Overlay of DRI chromatograms for Advantage polypropylene.

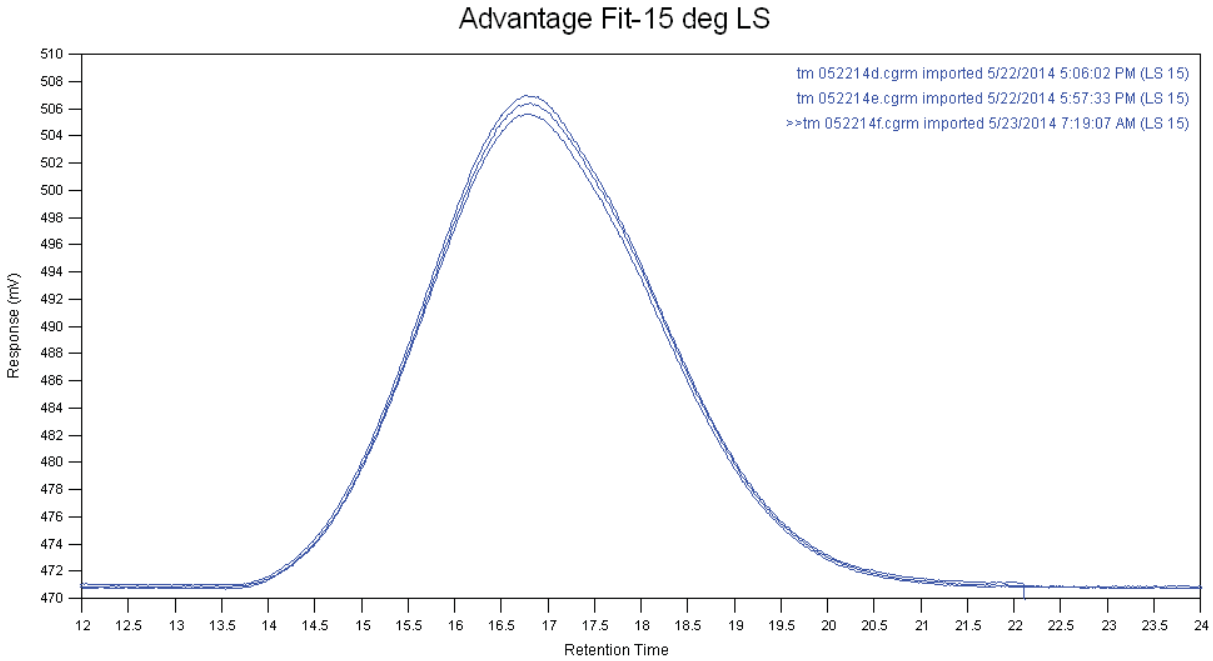

Figure S 10: Overlay of 15 degree light scattering chromatograms for Advantage polypropylene.

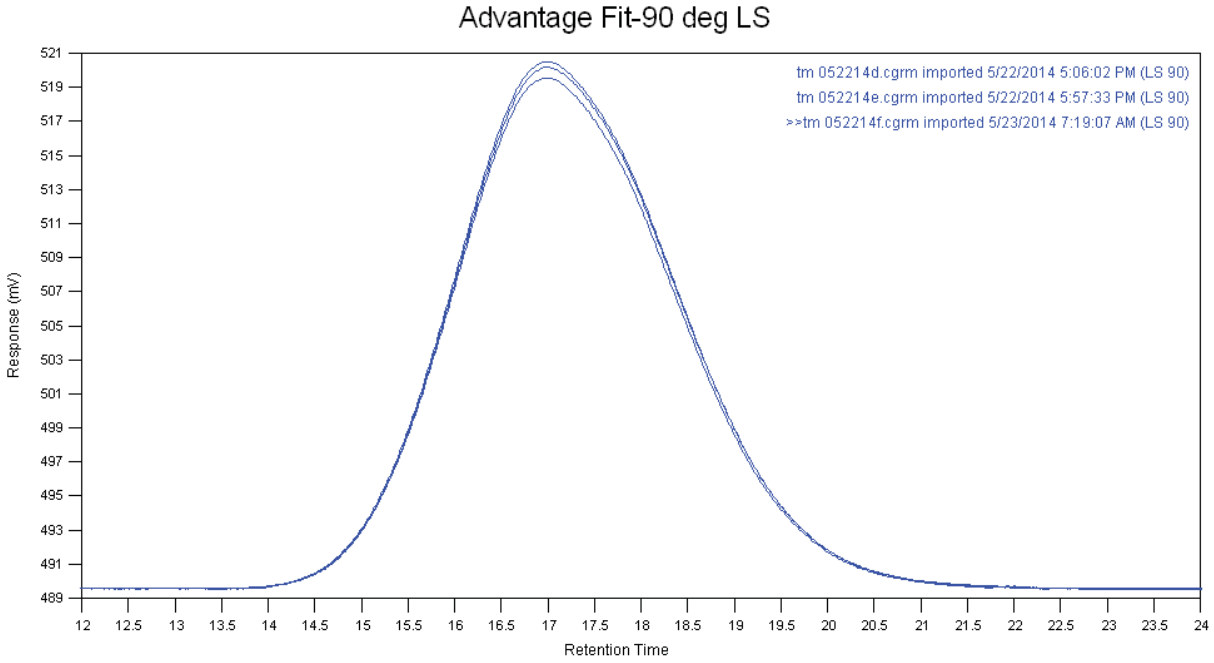

Figure S 12: Overlay of 90 degree light scattering chromatograms for Advantage polypropylene.

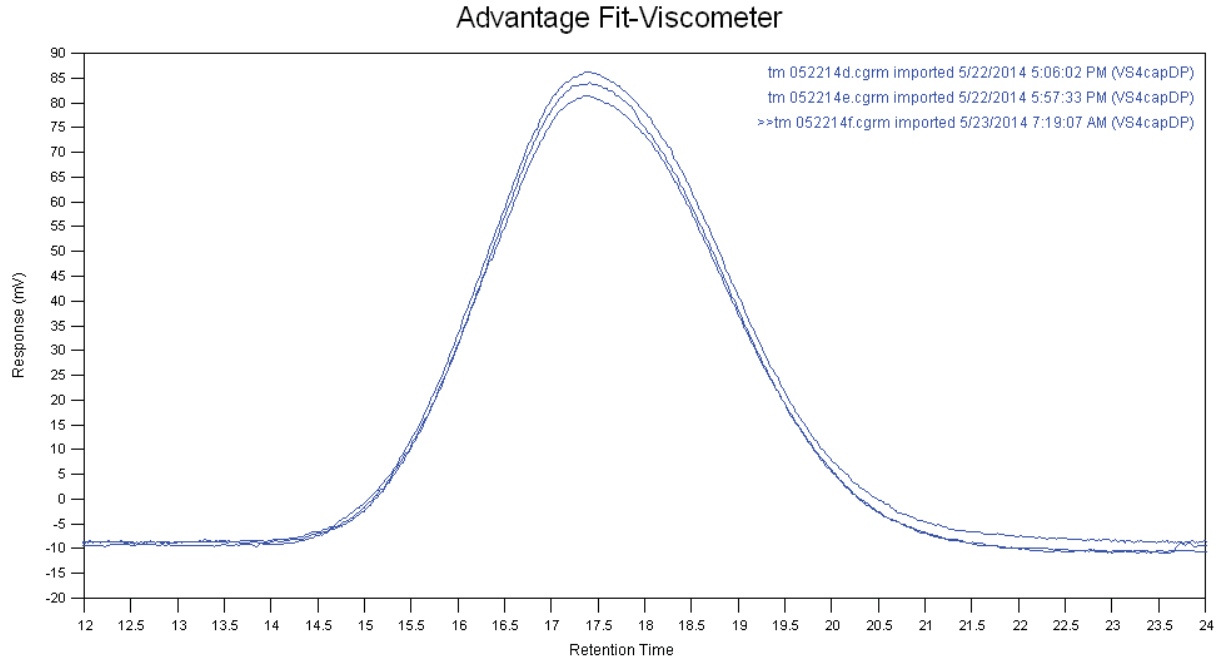

Figure S 13: Viscometer chromatograms for Advantage polypropylene.

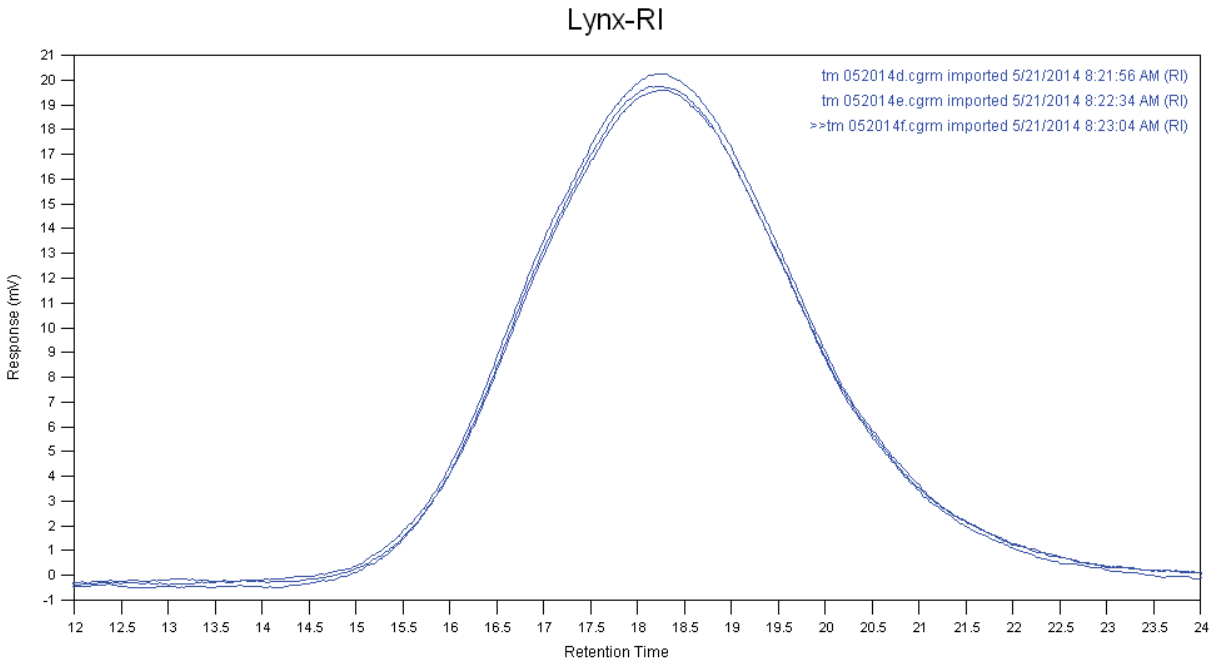

Figure S 14: DRI chromatograms for Lynx polypropylene.

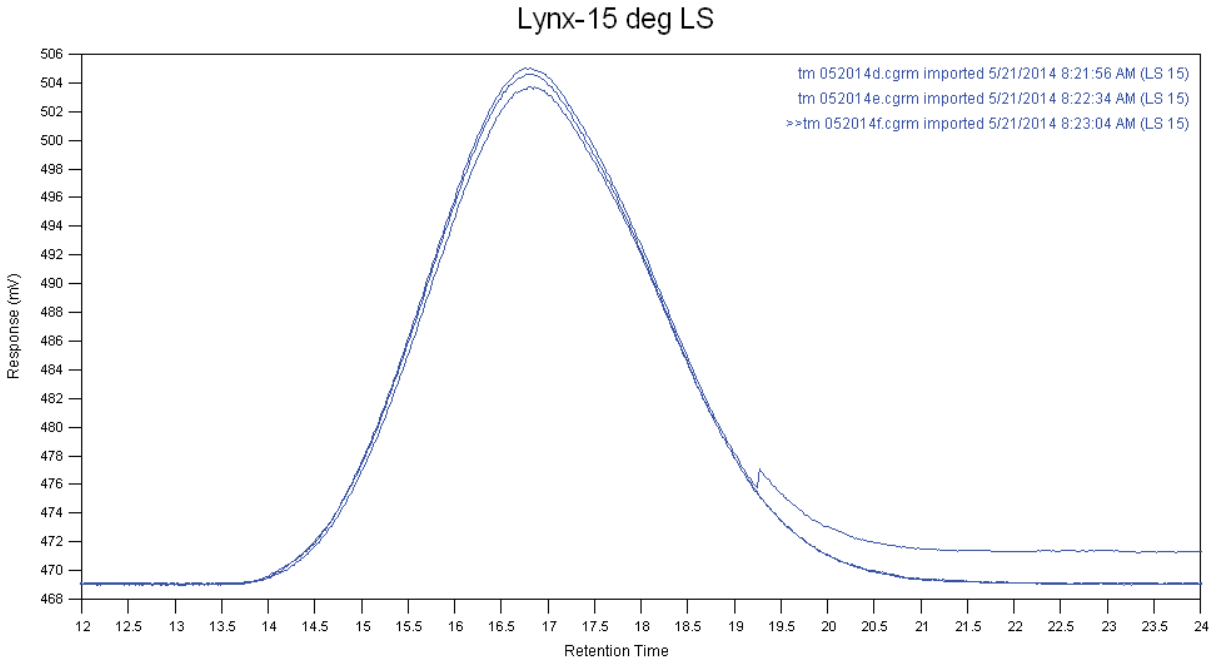

Figure S 15: 15 degree light scattering chromatograms for Lynx polypropylene.

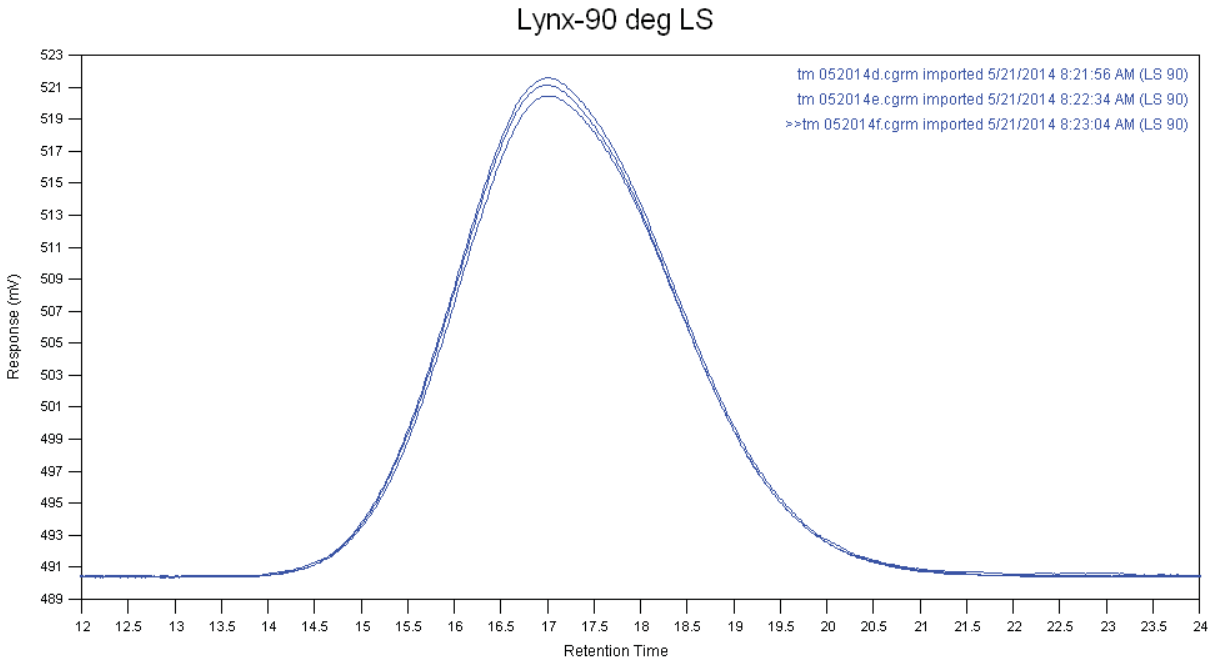

Figure S 16: 90 degree light scattering chromatograms for Lynx polypropylene.

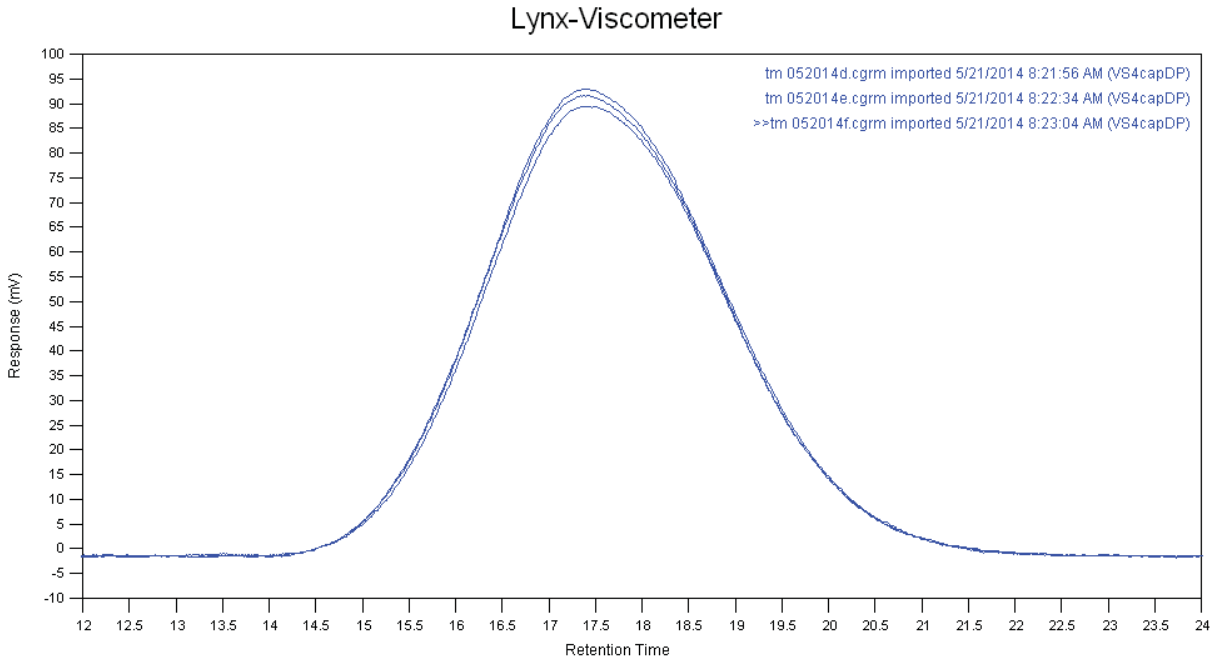

Figure S 17: Viscometer chromatograms for Lynx polypropylene.

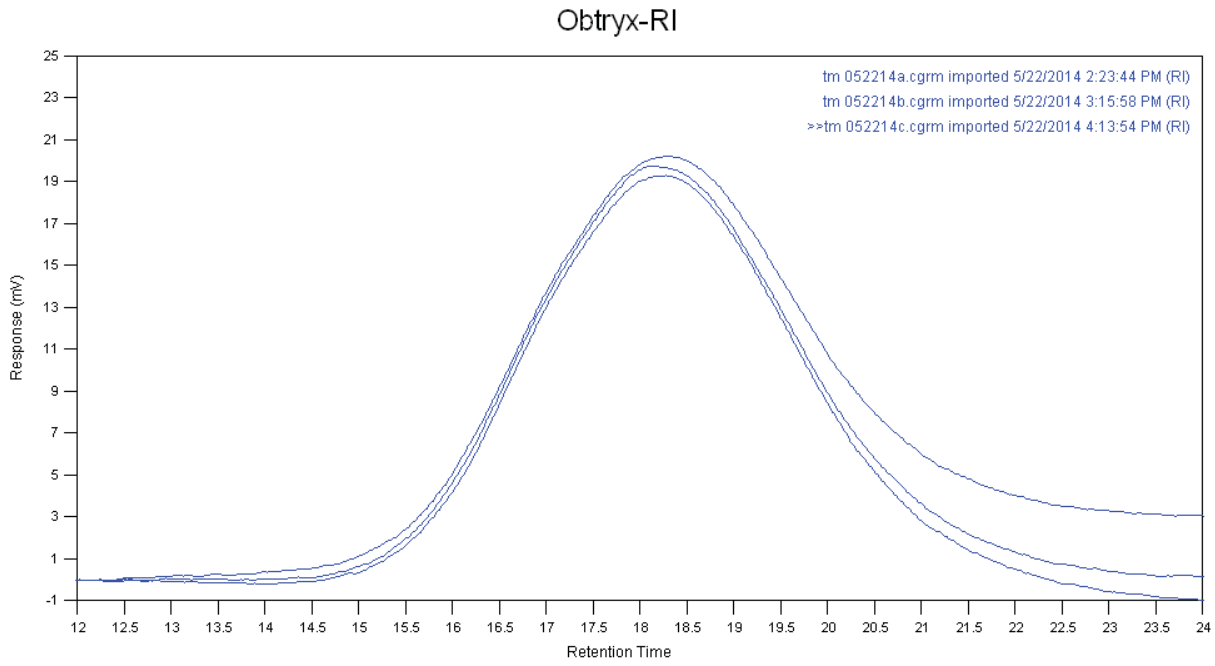

Figure S 18: DRI chromatograms for Obtryx polypropylene.

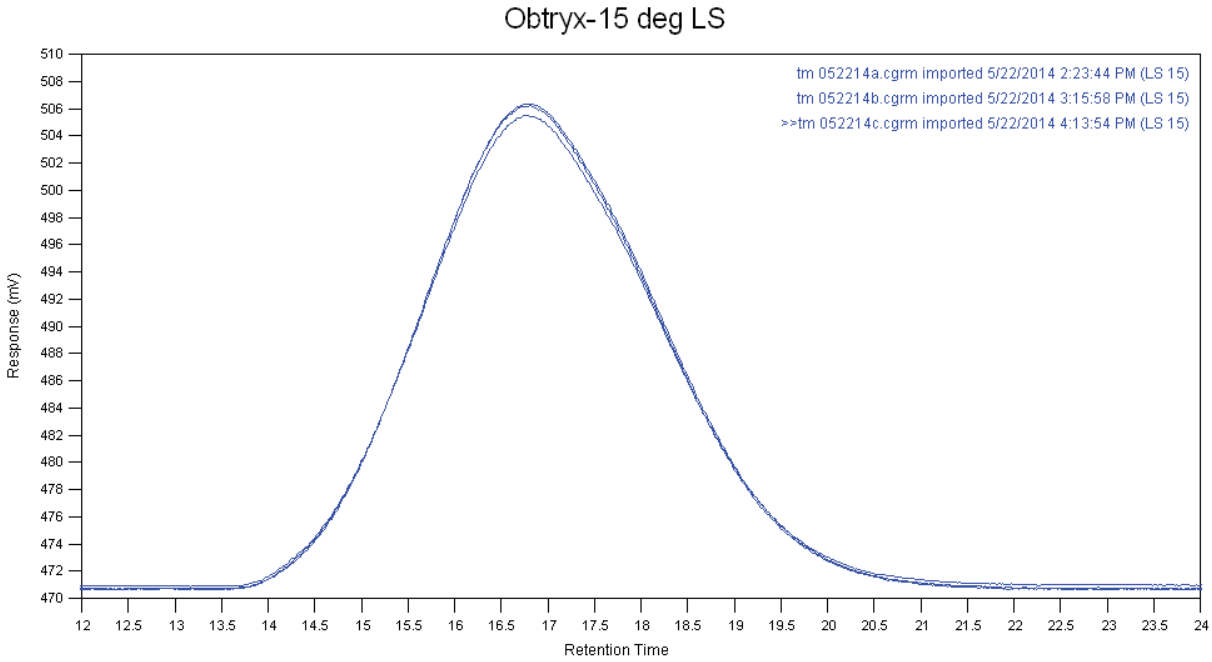

Figure S 19: 15 degree light scattering chromatograms for Obtryx polypropylene.

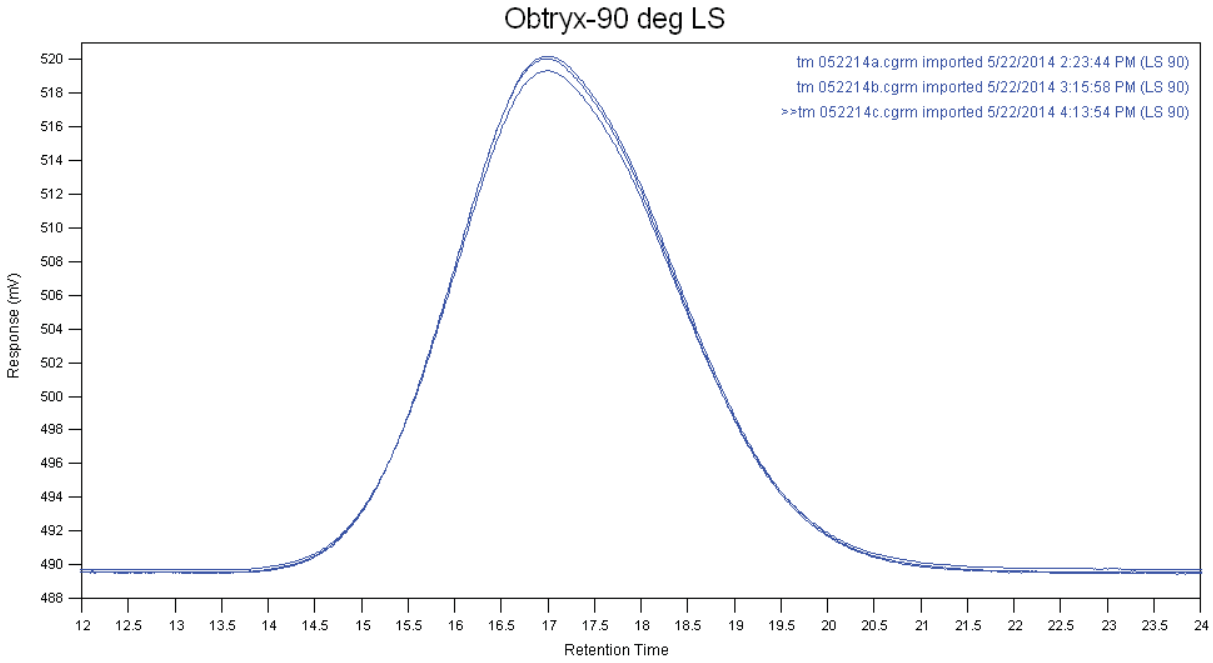

Figure S 20: 90 degree light scattering chromatograms for Obtryx polypropylene.

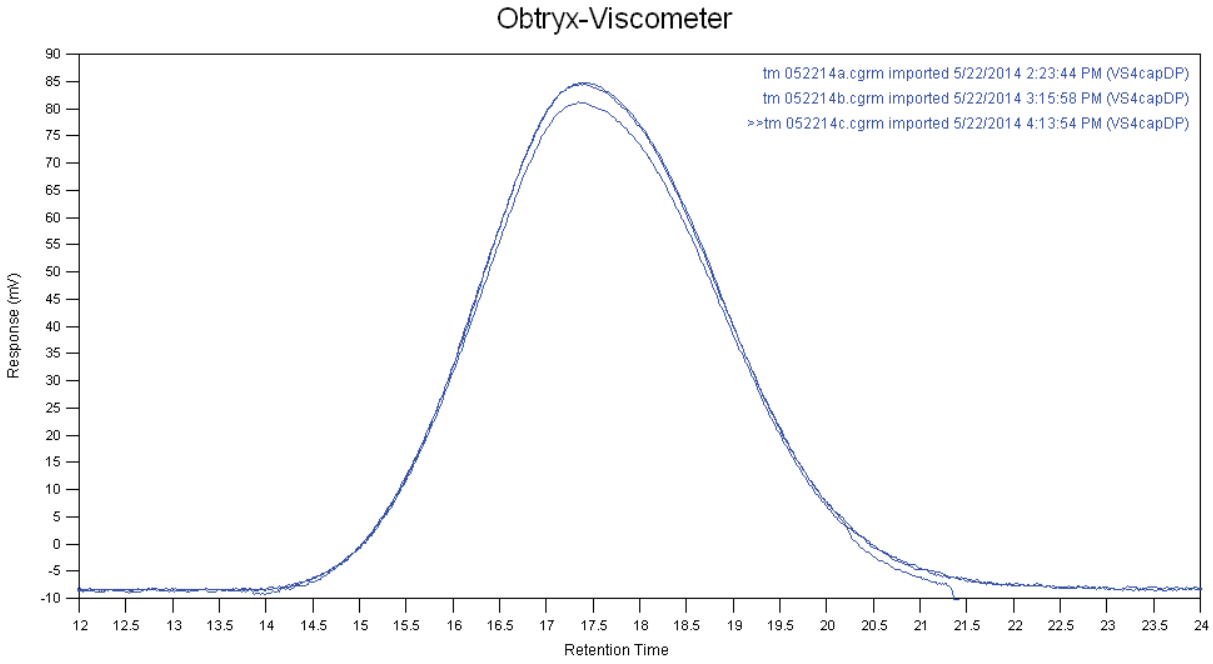

Figure S 21: Viscometer chromatograms for Obtryx polypropylene.

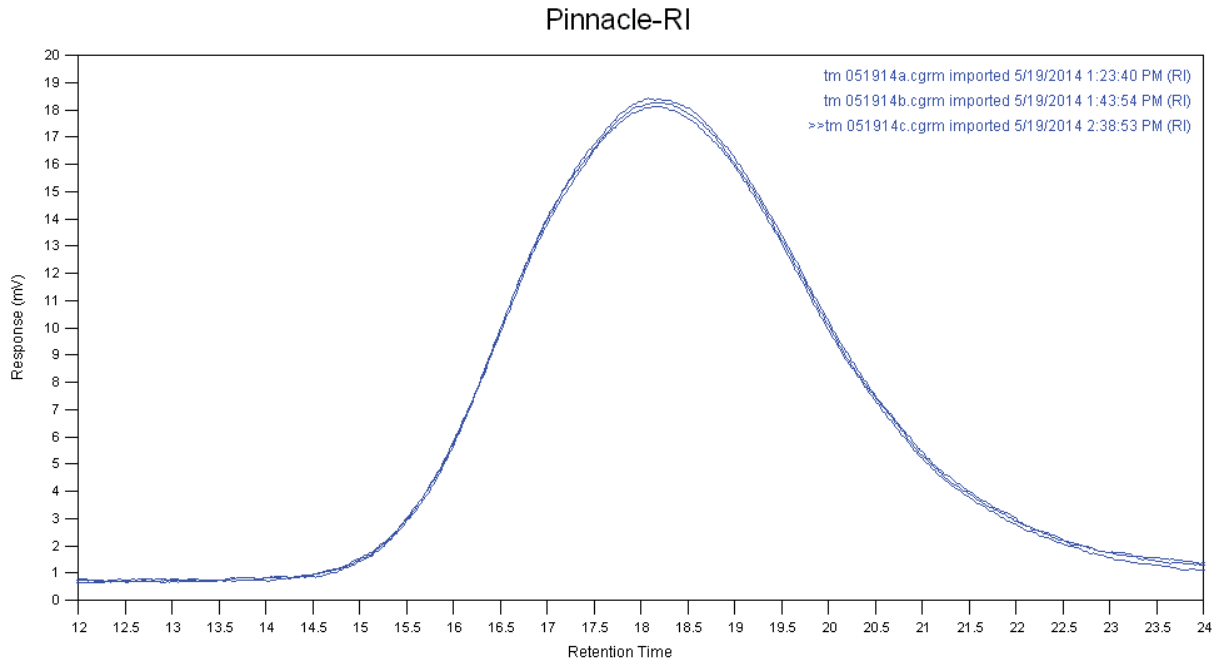

Figure S 22: DRI chromatograms for Pinnacle polypropylene.

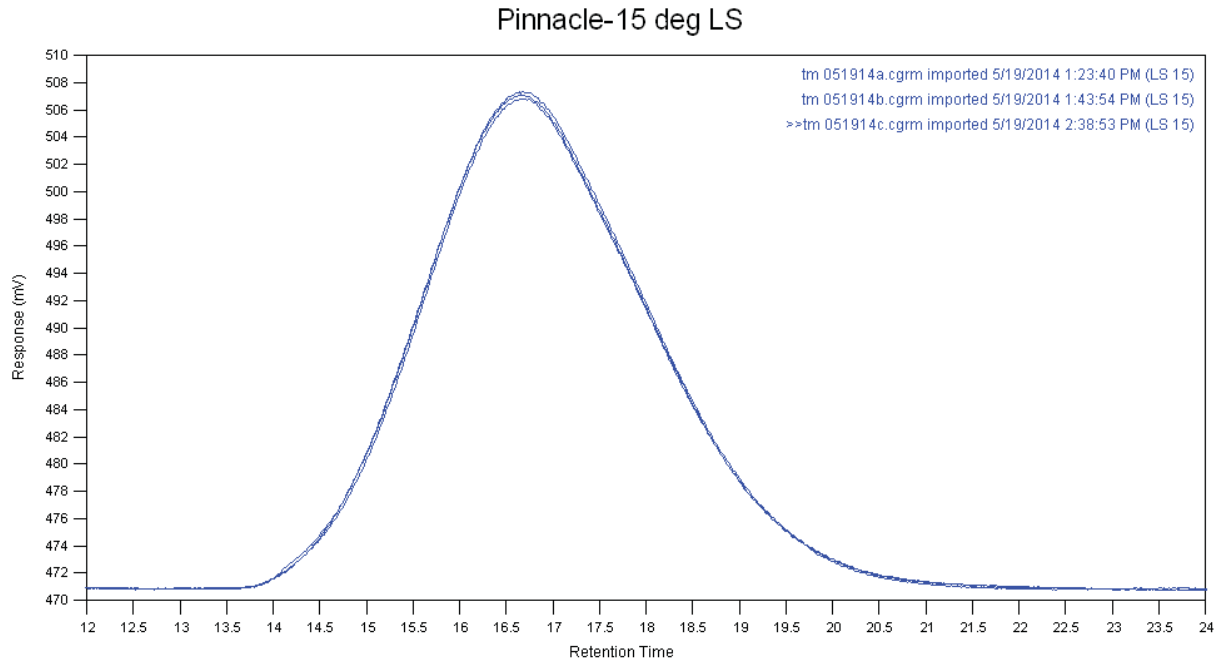

Figure S 23: 15 degree light scattering chromatograms for Pinnacle polypropylene.

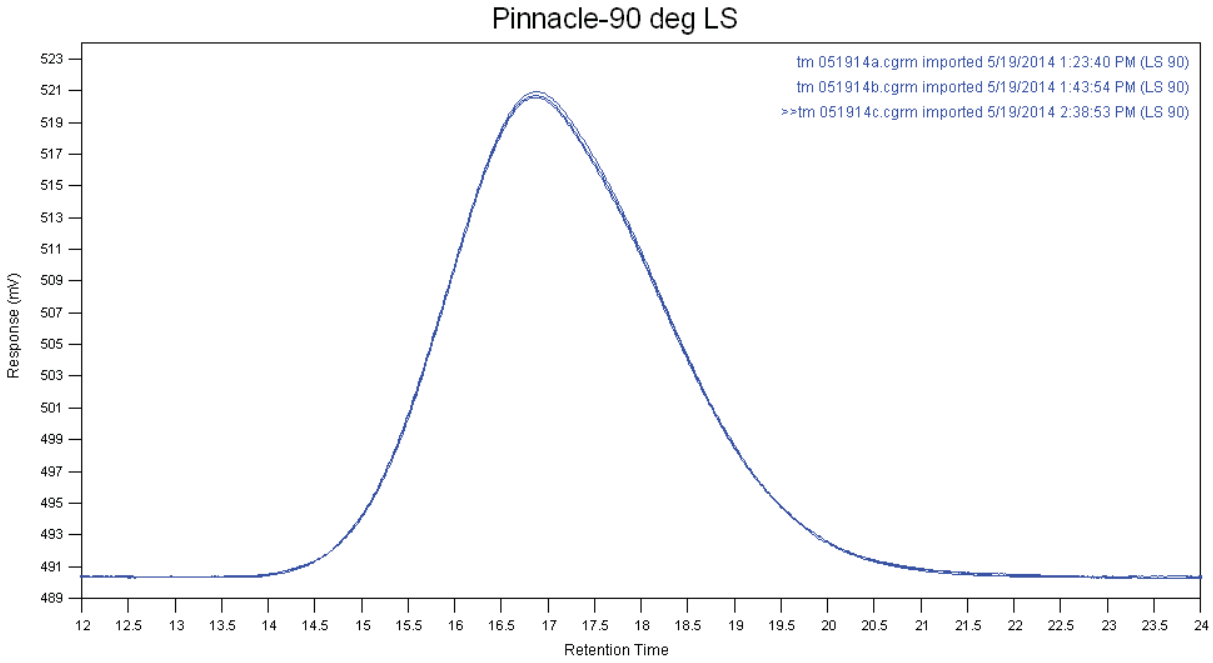

Figure S 256: 90 degree light scattering chromatograms for Pinnacle polypropylene.

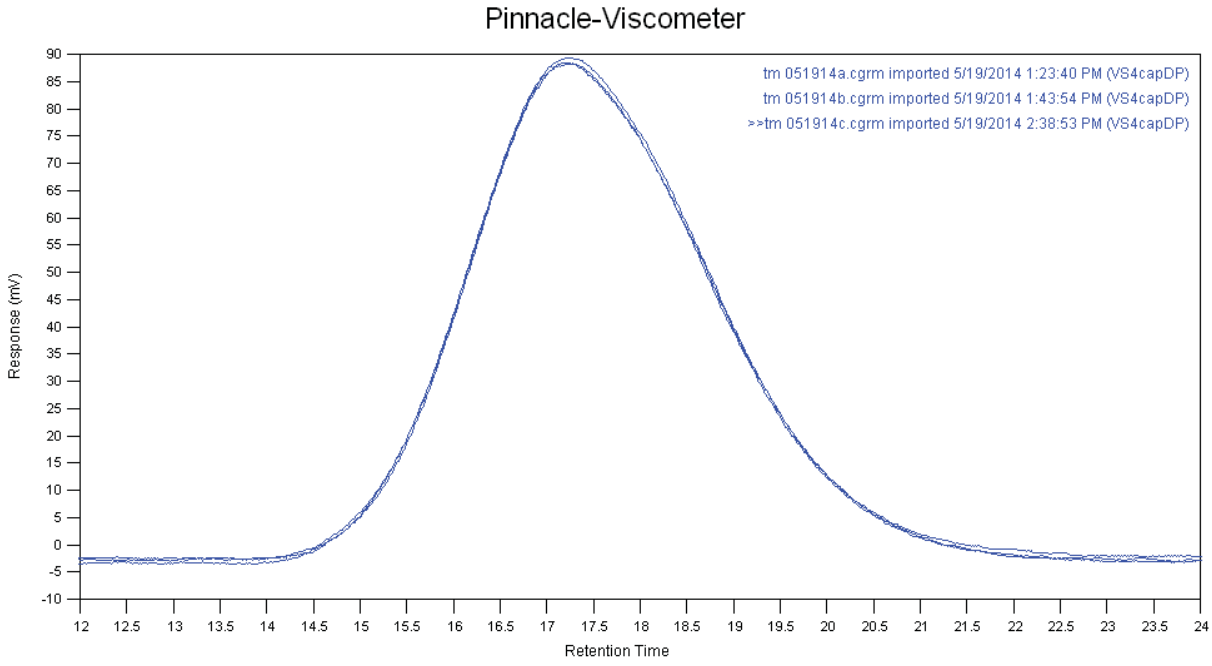

Figure S 247: Viscometer chromatograms for Pinnacle polypropylene.

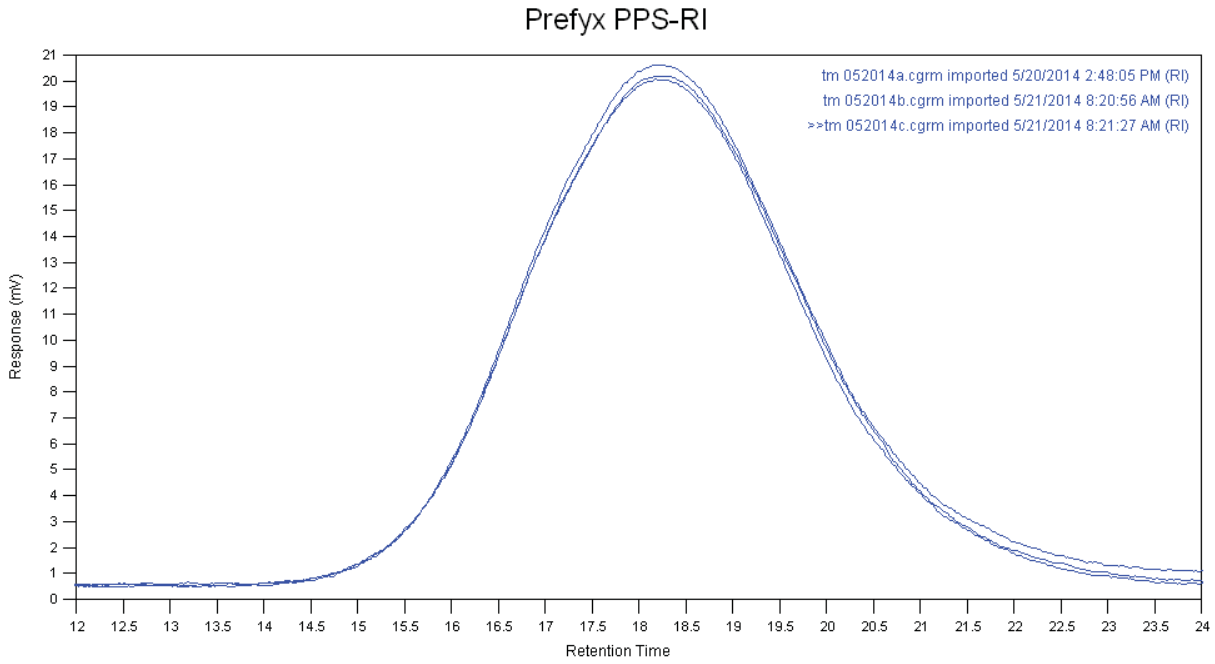

Figure S 26: DRI chromatograms for Prefyx polypropylene.

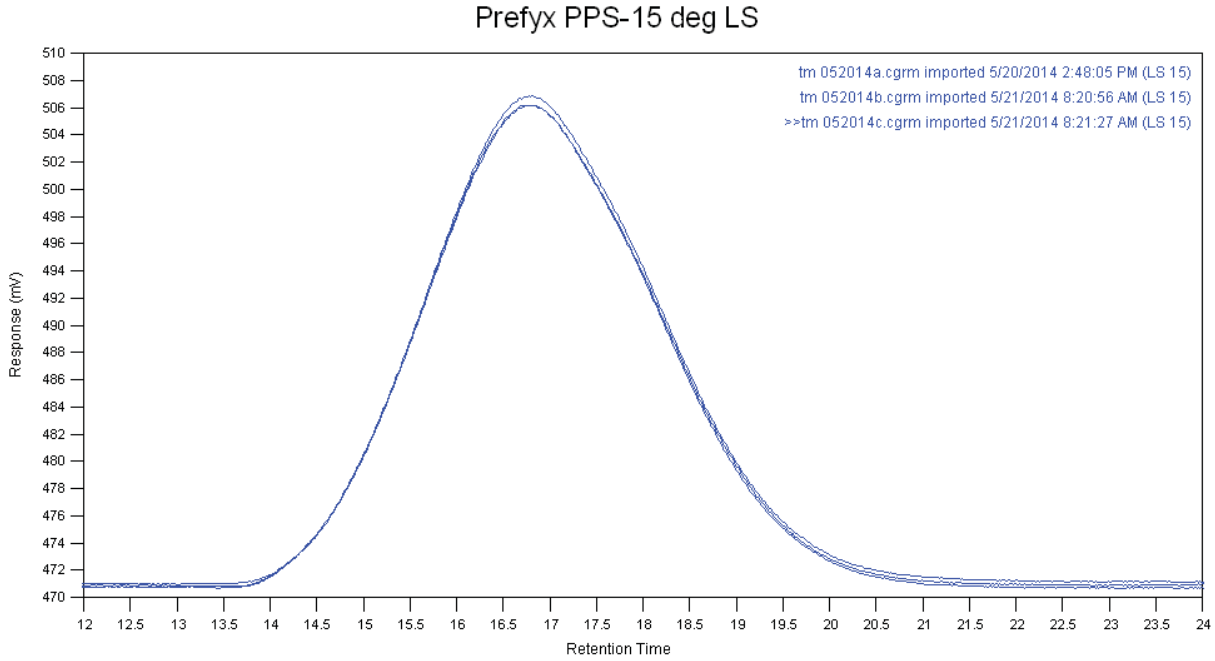

Figure S 27: 15 degree light scattering chromatograms for Prefyx polypropylene.

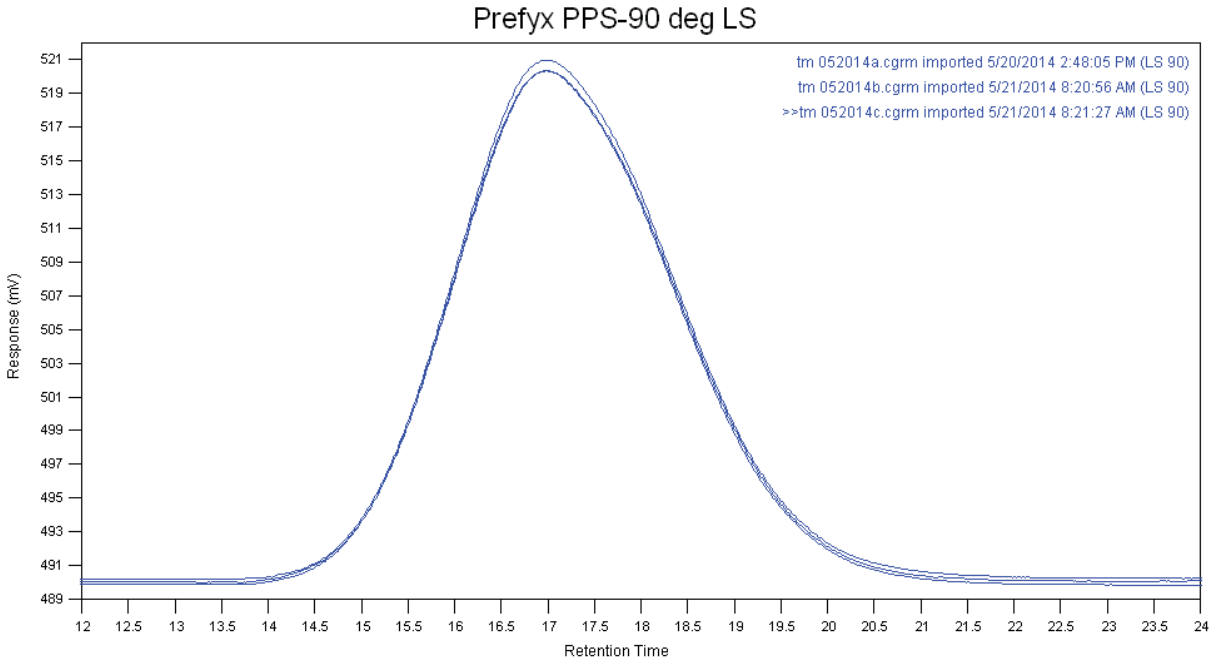

Figure S 28: 90 degree light scattering chromatograms for Prefyx polypropylene.

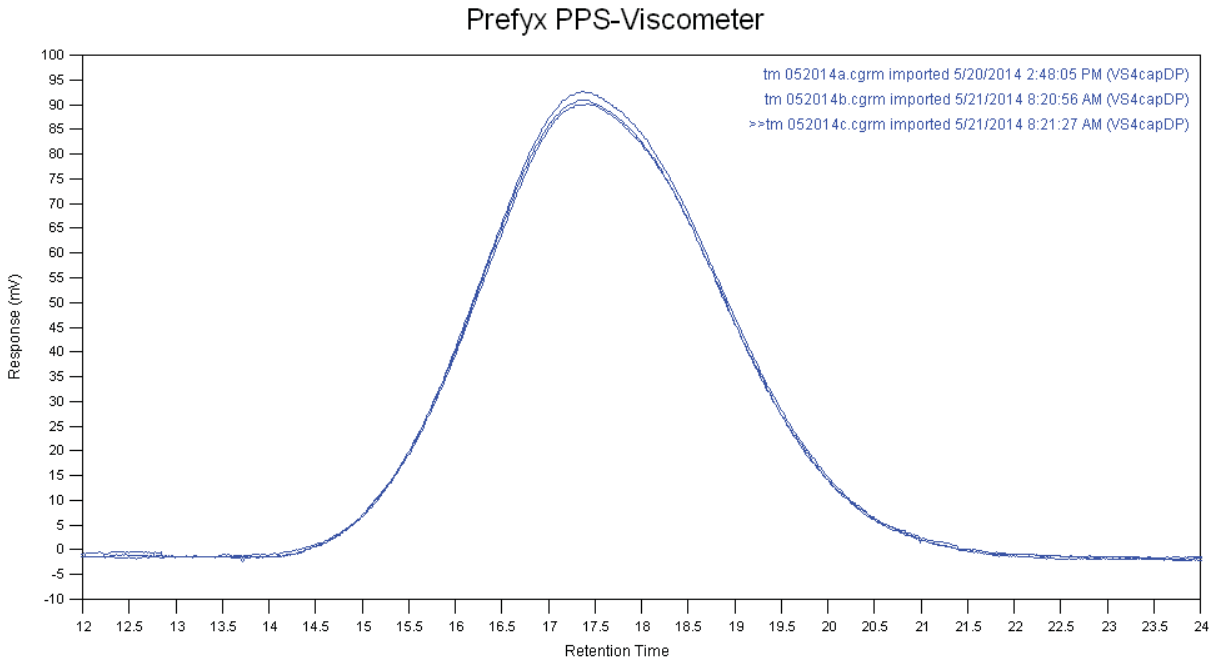

Figure S 29: Viscometer chromatograms for Prefyx polypropylene.

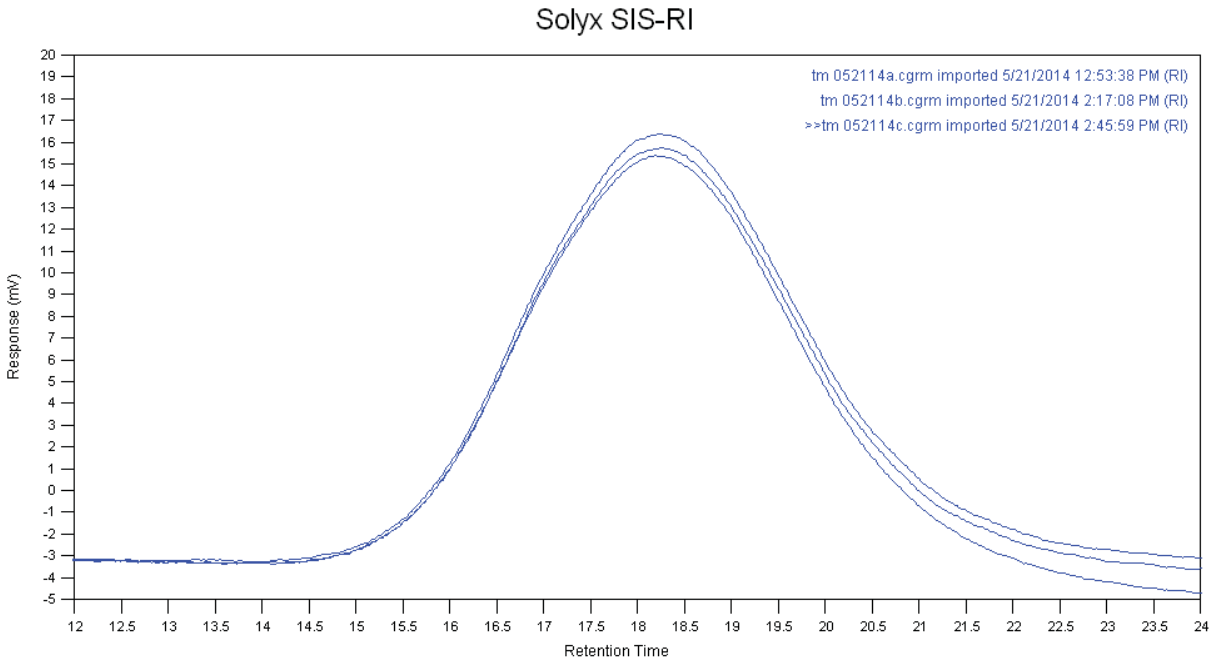

Figure S 30: DRI chromatograms for Solyx polypropylene.

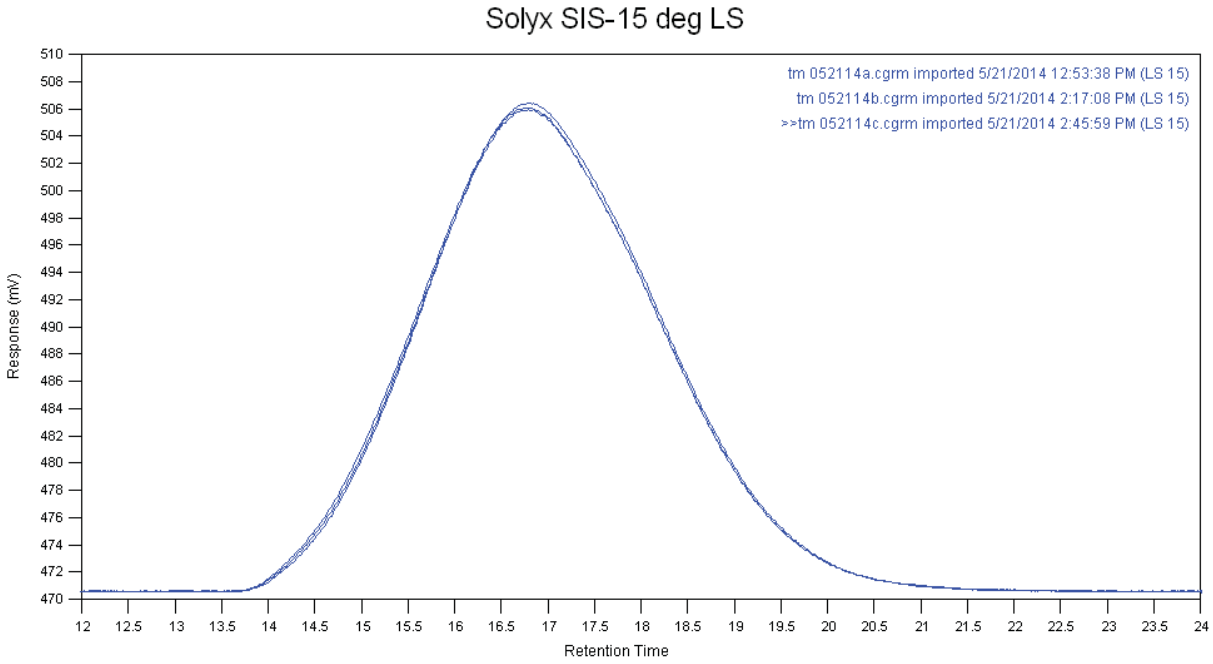

Figure S 31: 15 degree light scattering chromatograms for Solyx polypropylene.

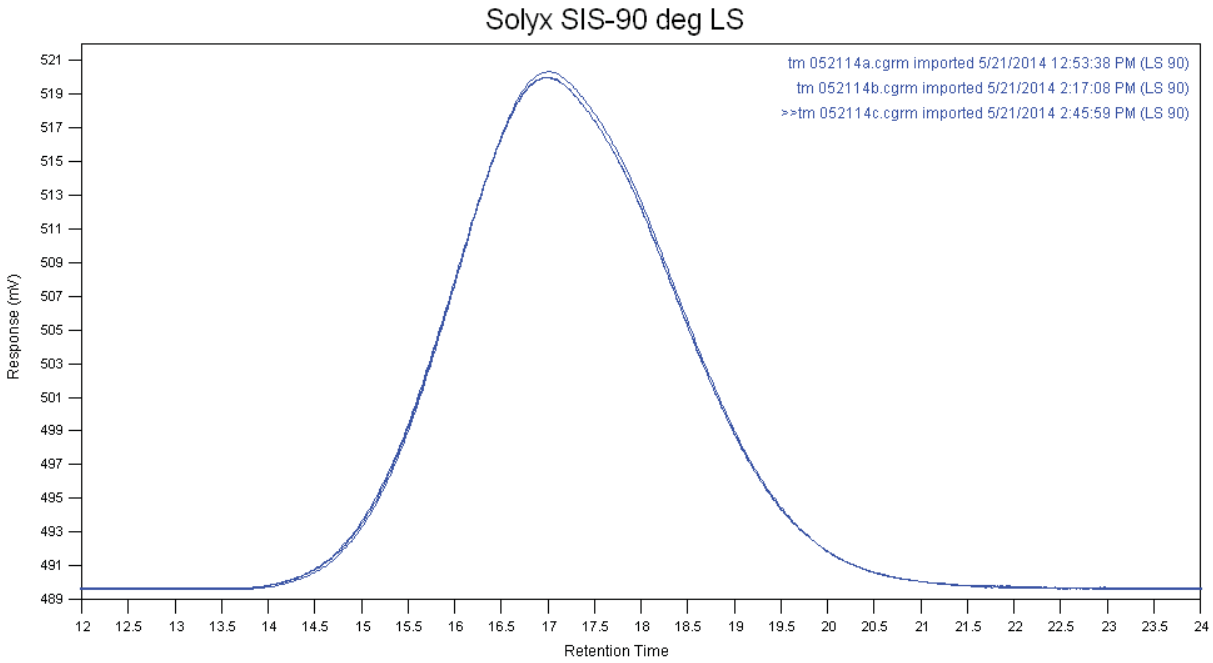

Figure S 32: 90 degree light scattering chromatograms for Solyx polypropylene.

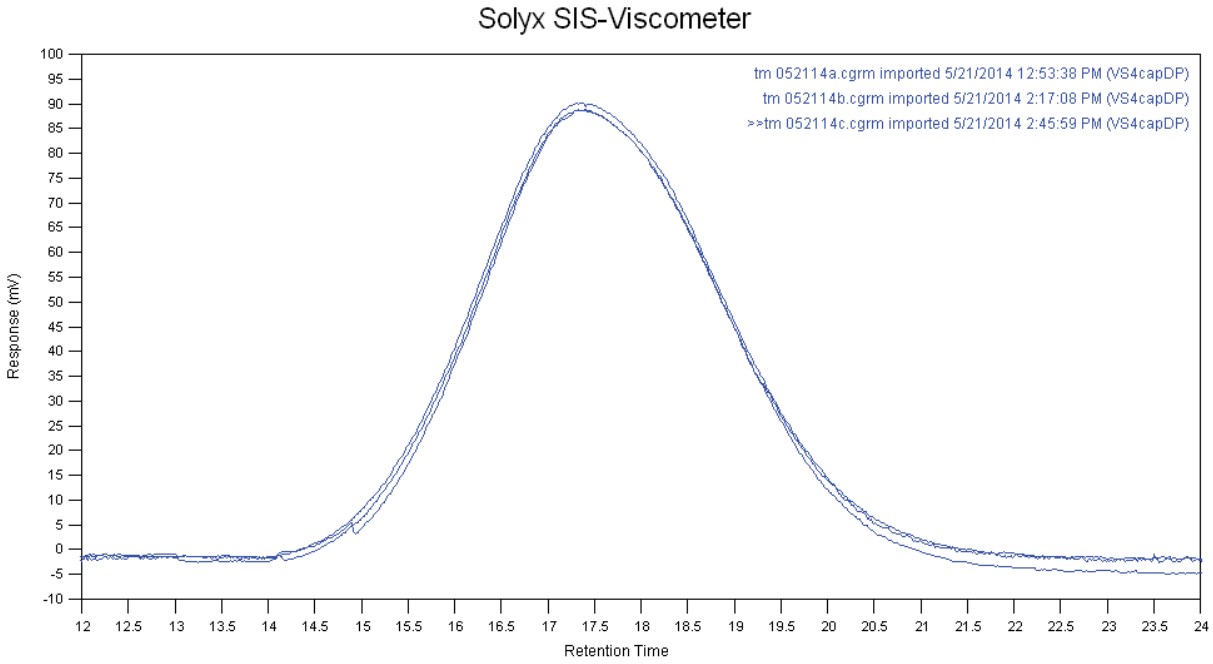

Figure S 33: Viscometer chromatograms for Solyx polypropylene.

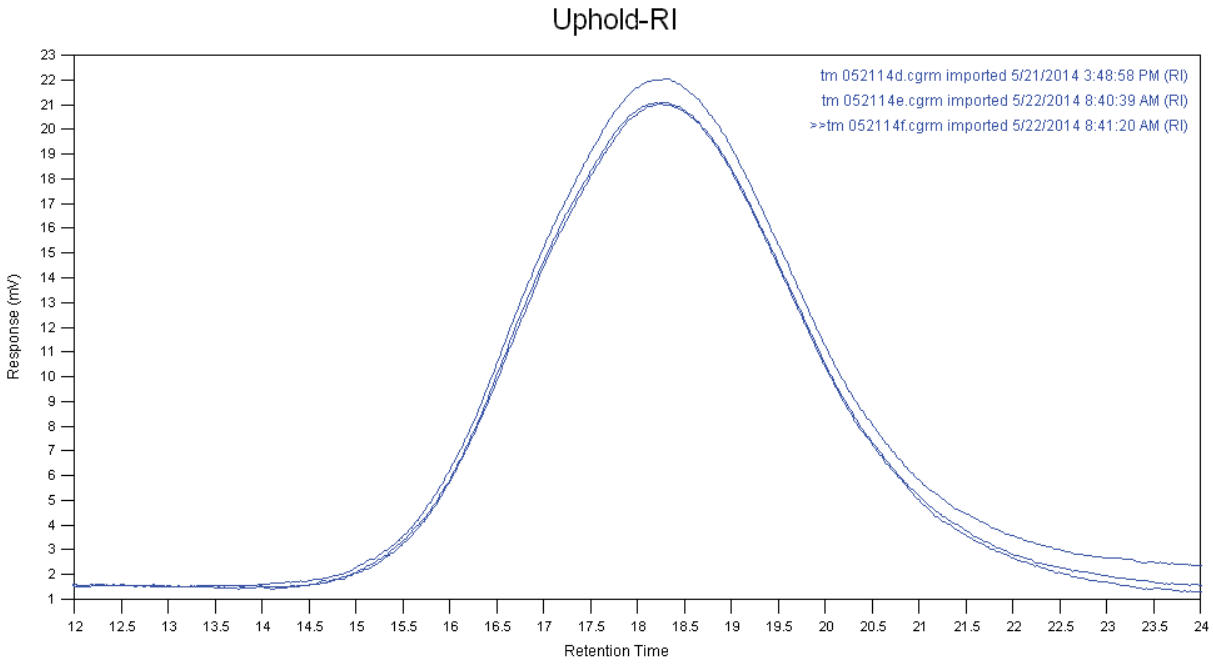

Figure S 34: DRI chromatograms for Uphold polypropylene.

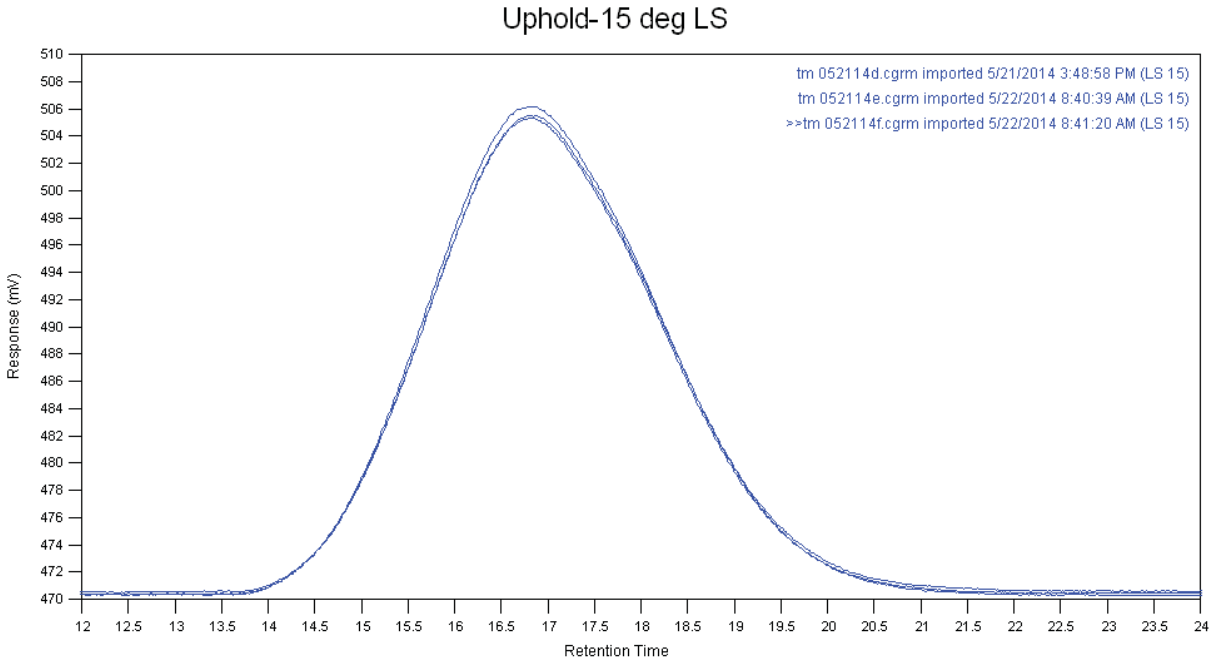

Figure S 35: 15 degree light scattering chromatograms for Uphold polypropylene.

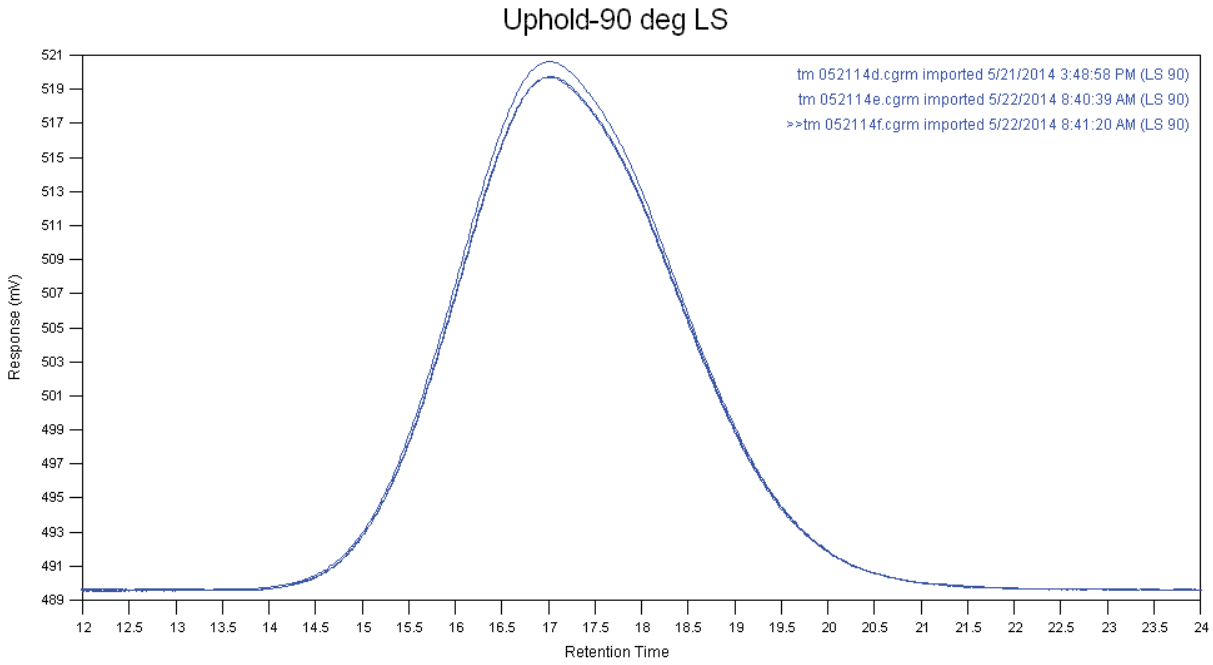

Figure S 36: 90 degree light scattering chromatograms for Uphold polypropylene.

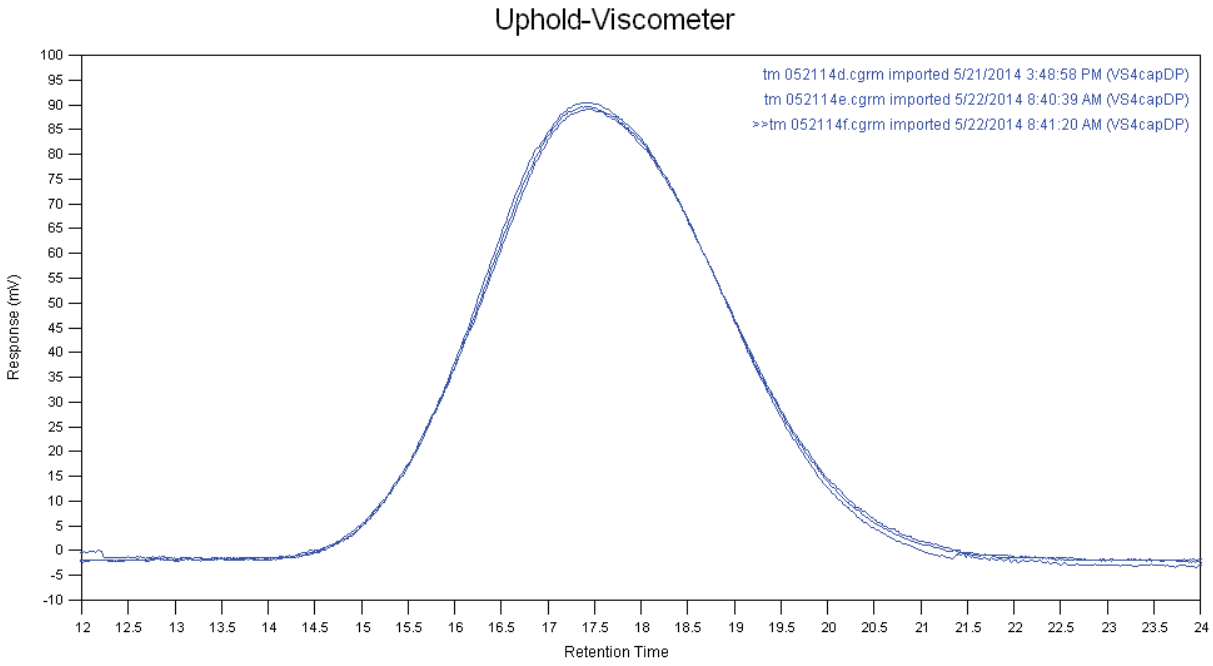

Figure S 37: Viscometer chromatograms for Uphold polypropylene.

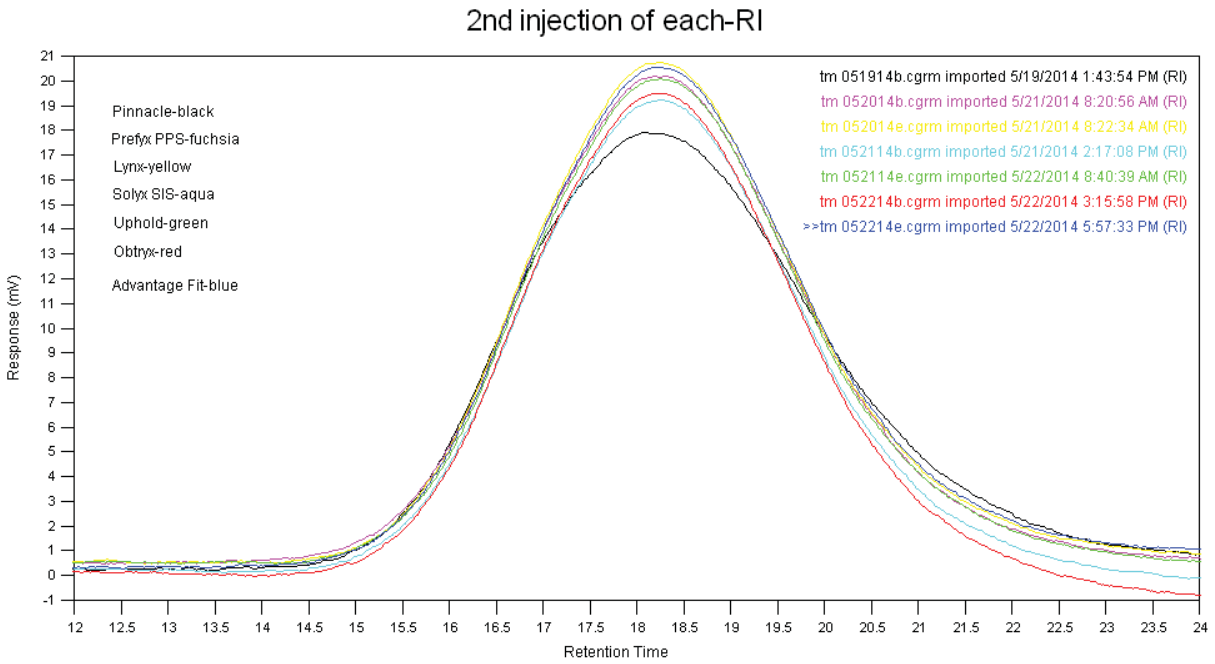

Figure S 38: Overlay of DRI chromatograms of each polypropylene mesh.

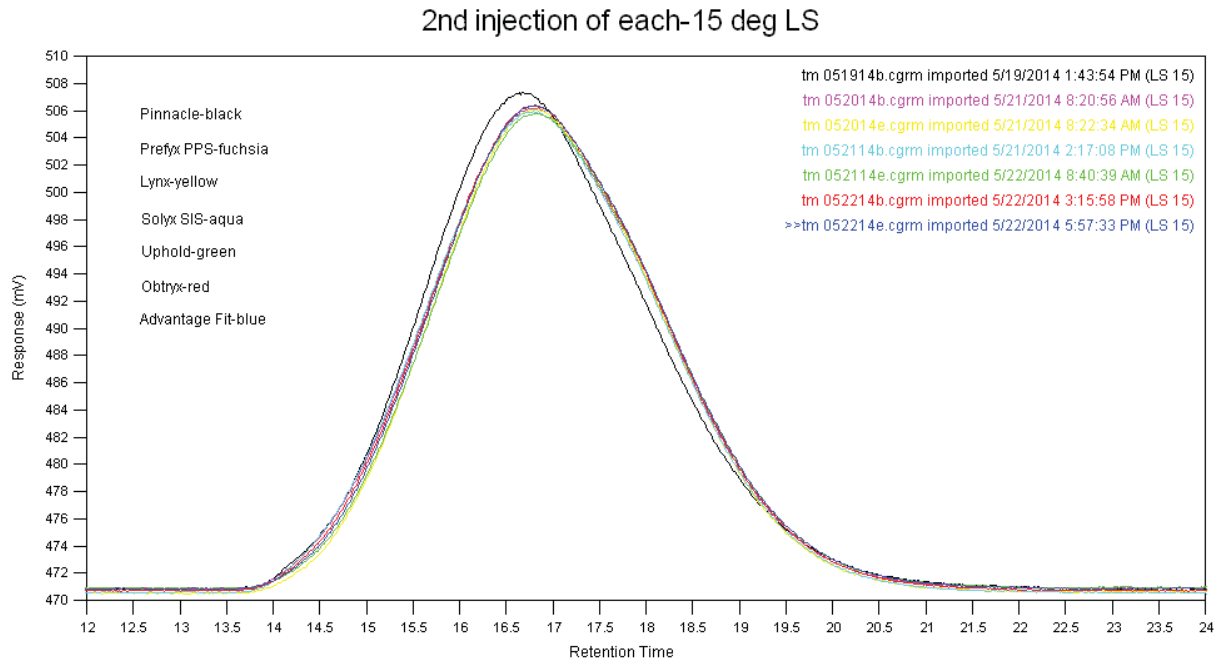

Figure S 39: Overlay of 15 degree light scattering chromatograms of each polypropylene mesh.

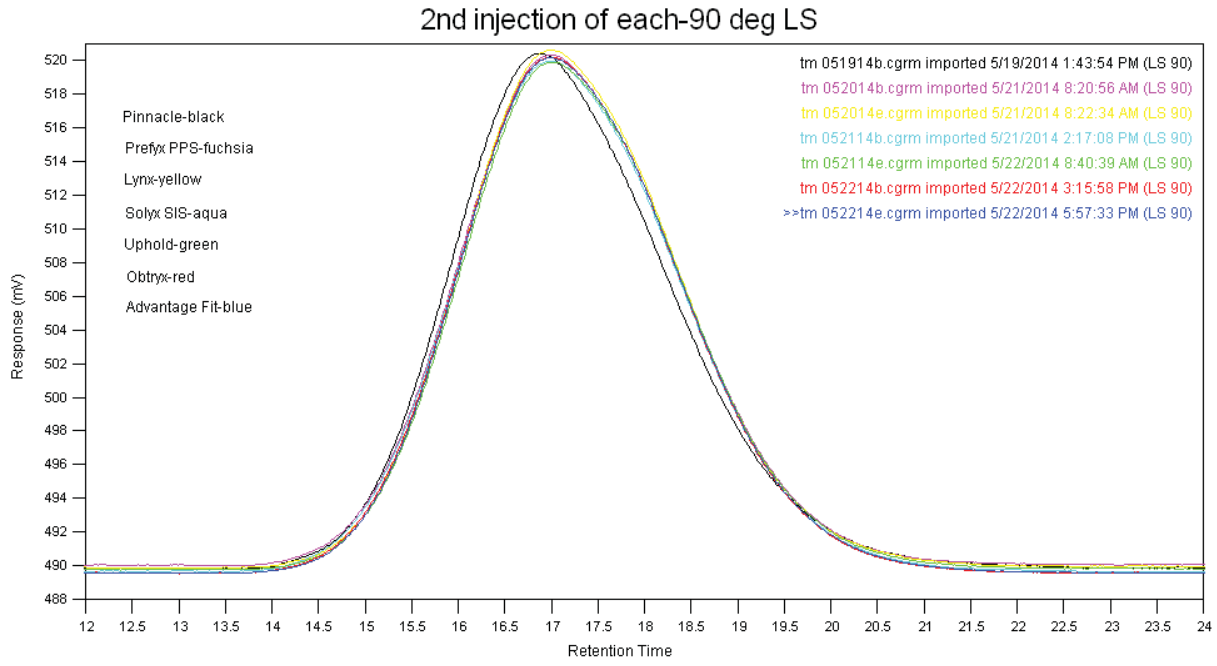

Figure S 40: Overlay of 90 degree light scattering chromatograms of each polypropylene mesh.

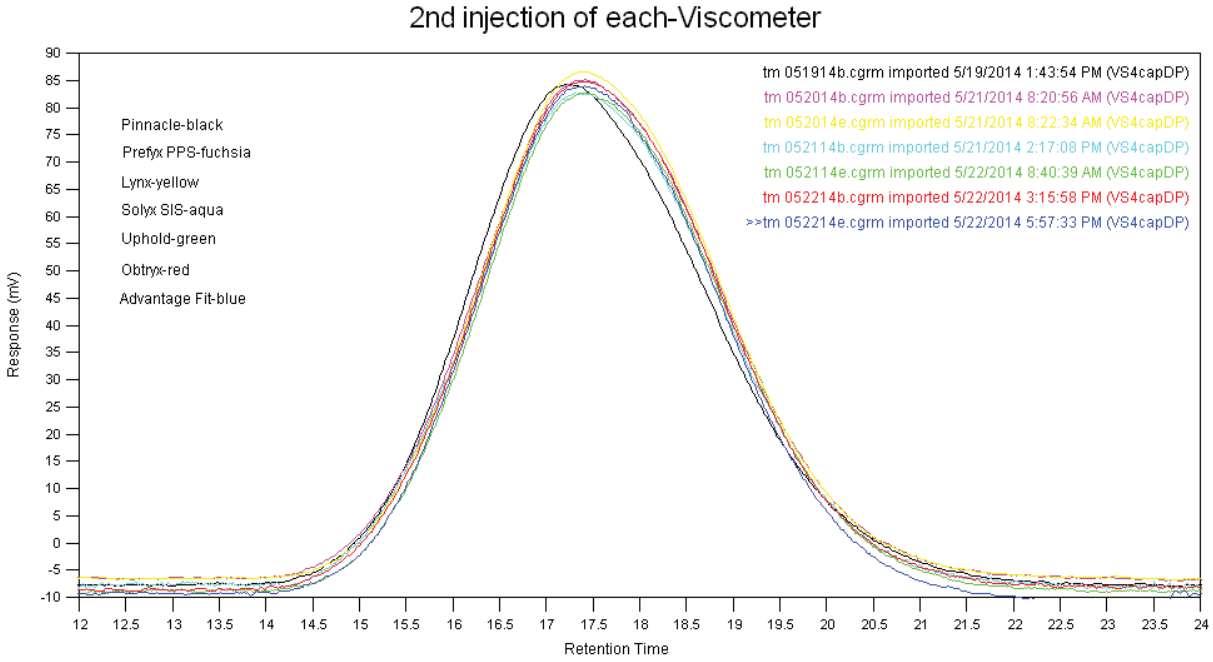

Figure S 41: Overlay of viscometer chromatograms of each polypropylene mesh.

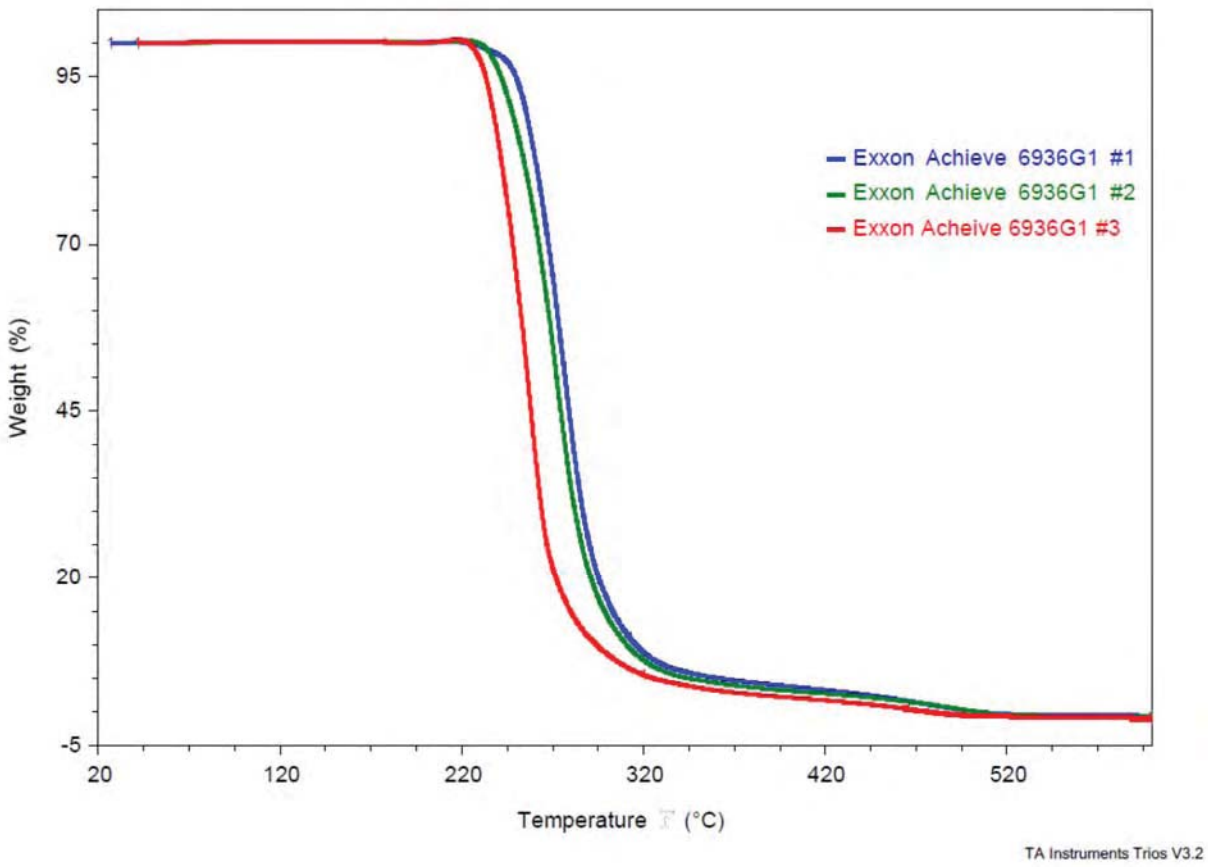

Figure S 42: TGA curves for Exxon Achieve 6936G1 polypropylene.